

This discussion paper is/has been under review for the journal Atmospheric Chemistry and Physics (ACP). Please refer to the corresponding final paper in ACP if available.

Recent variability of the solar spectral irradiance and its impact on climate modelling

I. Ermolli¹, K. Matthes², T. Dudok de Wit³, N. A. Krivova⁴, K. Tourpali⁵, M. Weber⁶, Y. C. Unruh⁷, L. Gray⁸, U. Langematz⁹, P. Pilewskie¹⁰, E. Rozanov^{11,12}, W. Schmutz¹¹, A. Shapiro¹¹, S. K. Solanki^{3,13}, G. Thuillier¹⁴, and T. N. Woods¹⁰

¹INAF, Osservatorio Astronomico di Roma, Monte Porzio Catone, Italy

²Helmholtz-Zentrum für Ozeanforschung Kiel (GEOMAR), Kiel, Germany

³LPC2E, CNRS and University of Orléans, Orléans, France

⁴Max-Planck-Institut für Sonnensystemforschung, 37191 Katlenburg-Lindau, Germany

⁵Laboratory of Atmospheric Physics, Aristotle University of Thessaloniki, Greece

⁶Institut für Umweltphysik, Universität Bremen FB1, Bremen, Germany

⁷Astrophysics Group, Blackett Laboratory, Imperial Collede London, SW7 2AZ, UK

⁸Centre for Atmospheric Sciences, Dept. of Atmospheric, Oceanic and Planetary Physics, University of Oxford, UK

⁹Institut für Meteorologie, Freie Universität Berlin, Berlin, Germany

¹⁰University of Colorado, Laboratory for Atmospheric and Space Physics, Boulder, CO, USA

[Title Page](#)

[Abstract](#)

[Introduction](#)

[Conclusions](#)

[References](#)

[Tables](#)

[Figures](#)

[◀](#)

[▶](#)

[◀](#)

[▶](#)

[Back](#)

[Close](#)

[Full Screen / Esc](#)

[Printer-friendly Version](#)

[Interactive Discussion](#)



¹¹Physikalisch-Meteorologisches Observatorium, World Radiation Center, Davos Dorf, Switzerland

¹²IAC ETH, Zurich, Switzerland

¹³School of Space Research, Kyung Hee University, Yongin, Gyeonggi 46-701, Republic of Korea

¹⁴LATMOS-IPSL, CNRS and University of Versailles-Saint-Quentin, Guyancourt, France

Received: 29 July 2012 – Accepted: 4 September 2012 – Published: 19 September 2012

Correspondence to: I. Ermolli (ilaria.ermolli@oa-roma.inaf.it)

Published by Copernicus Publications on behalf of the European Geosciences Union.

**Spectral irradiance
and climate**

I. Ermolli et al.

[Title Page](#)

[Abstract](#)

[Introduction](#)

[Conclusions](#)

[References](#)

[Tables](#)

[Figures](#)

[|◀](#)

[▶|](#)

[◀](#)

[▶](#)

[Back](#)

[Close](#)

[Full Screen / Esc](#)

[Printer-friendly Version](#)

[Interactive Discussion](#)



Abstract

During periods of high solar activity, the Earth receives $\approx 0.1\%$ higher total solar irradiance (TSI) than during low activity periods. Variations of the solar spectral irradiance (SSI) however, can be larger, with relative changes of 1 to 20 % observed in the ultraviolet (UV) band, and in excess of 100 % in the soft X-ray range. SSI changes influence the Earth's atmosphere, both directly, through changes in shortwave (SW) heating and therefore, temperature and ozone distributions in the stratosphere, and indirectly, through dynamical feedbacks. Lack of long and reliable time series of SSI measurements makes the accurate quantification of solar contributions to recent climate change difficult. In particular, the most recent SSI measurements show a larger variability in the UV spectral range and anomalous changes in the visible and near-infrared (NIR) bands with respect to those from earlier observations and from models. A number of recent studies based on chemistry-climate model (CCM) simulations discuss the effects and implications of these new SSI measurements on the Earth's atmosphere, which may depart from current expectations.

This paper summarises our current knowledge of SSI variability and its impact on Earth's climate. An interdisciplinary analysis of the topic is given. New comparisons and discussions are presented on the SSI measurements and models available to date, and on the response of the Earth's atmosphere and climate to SSI changes in CCM simulations. In particular, the solar induced differences in atmospheric radiative heating, temperature, ozone, mean zonal winds, and surface signals are investigated in recent simulations using atmospheric models forced with the current lower and upper boundaries of SSI solar cycle estimated variations from the NRLSSI model data and from SORCE/SIM measurements, respectively. Additionally, the reliability of available data is discussed and additional coordinated CCM experiments are proposed.

Spectral irradiance and climate

I. Ermolli et al.

[Title Page](#)

[Abstract](#)

[Introduction](#)

[Conclusions](#)

[References](#)

[Tables](#)

[Figures](#)

[◀](#)

[▶](#)

[◀](#)

[▶](#)

[Back](#)

[Close](#)

[Full Screen / Esc](#)

[Printer-friendly Version](#)

[Interactive Discussion](#)



1 Introduction

The question of whether – and to what extent – the Earth's climate is influenced by solar variability remains central to the understanding of anthropogenic climate change.

According to the 4th assessment report of the Intergovernmental Panel on Climate Change, about 8 % of recent global climate change may be attributed to solar variability (Solomon et al., 2007). However, there is a large uncertainty in this figure because several aspects of solar forcing and the different mechanisms by which solar variability influences the Earth's environment are still poorly understood (see e.g. Pap et al., 2004; Calisesi et al., 2007; Haigh, 2007; Gray et al., 2010; Lockwood, 2012, and references therein). For these reasons, the quantification of the solar contribution to climate change remains incomplete. This is further highlighted by some of the most recent investigations of Solar Spectral Irradiance (SSI) variations and estimates of their influence on the Earth's atmosphere based on chemistry-climate model (CCM) simulations.

Regular space-based measurements of the solar irradiance started in 1978 (see Sects. 2.1 and 2.3). The Total Solar Irradiance (TSI), i.e. the spectrally integrated radiative power density of the Sun incident at the top of Earth's atmosphere, has been monitored almost continuously and was found to vary on different time scales (Willson et al., 1981; Fröhlich and Lean, 2004; Fröhlich, 2009). Most pronounced is the $\approx 0.1\%$ modulation of TSI in phase with the 11-yr solar sunspot or activity cycle. Measurements of SSI, however, are not continuous over the satellite era and until recently have concentrated on the ultraviolet (UV) radiation, because of the larger relative variability of SSI below 400 nm and the impact of these wavelengths on the terrestrial atmosphere through radiative heating and ozone photochemistry (Fig. 1).

SSI variations differ from those observed in the TSI. The variability of visible and NIR bands barely exceeds 0.5 % over a solar cycle; in the near UV and shorter wavelengths variability increases with decreasing wavelength, reaching several percent at 200–250 nm, and several tens of percent, or even more, below about 200 nm (e.g. Floyd et al., 2003, and references therein). Because it is almost completely absorbed

[Title Page](#)

[Abstract](#)

[Introduction](#)

[Conclusions](#)

[References](#)

[Tables](#)

[Figures](#)

[◀](#)

[▶](#)

[◀](#)

[▶](#)

[Back](#)

[Close](#)

[Full Screen / Esc](#)

[Printer-friendly Version](#)

[Interactive Discussion](#)



in the Earth's atmosphere (Fig. 1), solar UV radiation between 120 and 350 nm is the primary agent affecting heating, photochemistry, and therefore, the dynamics of the Earth's atmosphere. Variations of solar UV lead to changes in stratospheric ozone and heating, and hence to indirect amplification of solar UV forcing. Therefore, although the 5 UV radiation represents less than 8 % of the TSI (Krivova et al., 2006), its variability may have a significant impact on climate. In contrast, the visible and IR bands have the largest contribution to the TSI and directly heat Earth's surface and lower atmosphere. Their impact on the Earth's climate is expected to be small unless it involves amplification mechanisms (e.g. the "bottom-up" mechanism, van Loon et al., 2007, see also 10 Sect. 4.1).

Early satellite measurements of the solar UV variability have shown a qualitatively consistent behaviour (Deland and Cebula, 2012), which is fairly well reproduced by SSI models (e.g. Lean et al., 1997; Krivova et al., 2006; Unruh et al., 2012; Lean and DeLand, 2012); see Fig. 2. This situation changed with the launch of the Spectral Irradiance Monitor instrument (SIM, Harder et al., 2005a) onboard the Solar Radiation and Climate Experiment satellite (SORCE, Rottman, 2005) in 2003, which was shortly after 15 the most recent maximum of solar activity. The SORCE/SIM data showed a four to six times greater decrease of the UV radiation between 200 and 400 nm over the period 2004–2008 (Harder et al., 2009), part of the declining phase of solar cycle 23, compared to earlier measurements and models (Ball et al., 2011; Pagaran et al., 2011a; 20 Unruh et al., 2012; Deland and Cebula, 2012; Lean and DeLand, 2012). This larger decrease measured in the UV (Fig. 2), which exceeds the TSI decrease over the same period by almost a factor of two, is compensated by an increase in the visible and NIR bands. Variability out-of-phase with solar activity is indeed predicted by some SSI models 25 in the NIR (see Sects. 3.3 and 3.4), but with a significantly lower magnitude than found by SORCE/SIM (Fig. 2).

When used as solar input to CCM simulations, SORCE/SIM observations lead to significantly larger SW heating rates in the upper stratosphere compared to results obtained by using the commonly utilized NRLSSI model data (Lean et al., 1997; Lean,

[Title Page](#)[Abstract](#)[Introduction](#)[Conclusions](#)[References](#)[Tables](#)[Figures](#)[|◀](#)[▶|](#)[◀](#)[▶](#)[Back](#)[Close](#)[Full Screen / Esc](#)[Printer-friendly Version](#)[Interactive Discussion](#)

2000, see Sect. 3), and a decrease of stratospheric ozone above an altitude of 45 km during solar maximum (Haigh et al., 2010). These changes in radiative heating and ozone photochemistry in the stratosphere also impact the responses of the “top-down” solar UV mechanism in the Earth’s atmosphere and at the surface (Kodera and Kuroda, 5 2002), which may depart from current understanding (Cahalan et al., 2010; Ineson et al., 2011; Merkel et al., 2011; Oberländer et al., 2012; Swartz et al., 2012). It is difficult to validate the results of these model simulations with ozone, zonal wind, or temperature measurements since the data are sparse and do not cover enough solar cycles. Although some ozone observations seem to agree with model calculations (e.g. 10 Haigh et al., 2010; Merkel et al., 2011), it should be noted that the SIM measurements available covered less than one solar cycle, requiring extrapolation over a full cycle, and therefore, adding uncertainty (Garcia, 2010). Also the transition altitude from in-phase (lower and middle stratosphere) to out-of-phase (upper stratosphere) ozone signals with the solar cycle is not consistent among the different models and requires further 15 investigations.

Unfortunately, observations of the full solar spectrum will likely have a multi-year gap before the next generation SSI instrument is launched. Based on data presently available, a thorough understanding of the impact of SSI on climate requires verification and validation of existing SSI measurements for internal consistency, calculations of 20 middle atmosphere climate models with different reliable scenarios of SSI variations, and comparison of measurements and model results with climate records, i.e. a study involving the coordinated work of various research communities. This objective is part of the COST Action ES1005¹ to which most of the authors of this paper belong.

This paper, which is the outcome of an interdisciplinary workshop in the frame of the 25 COST Action ES1005, summarizes and compares, for the first time, a large number of SSI observations and models, and discusses the impact of these data on Earth’s climate. Although the Sun affects the climate system in numerous ways, the focus is

¹TOSCA – towards a more complete assessment of the impact of solar variability on the Earth’s climate, <http://www.tosca-cost.eu>.

[Title Page](#)[Abstract](#)[Introduction](#)[Conclusions](#)[References](#)[Tables](#)[Figures](#)[◀](#)[▶](#)[◀](#)[▶](#)[Back](#)[Close](#)[Full Screen / Esc](#)[Printer-friendly Version](#)[Interactive Discussion](#)

on radiative forcing only, with particular attention given to the role of the SSI rather than that of the TSI, which is still the sole solar input in many climate models. Space-based observations of the SSI and of the terrestrial atmosphere conditions are sparse or absent before 1980, so we restrict our analysis to the data of the last three decades,
5 i.e. roughly the last three solar cycles. Furthermore, we concentrate on the effects of the UV variability because of its potentially large impact on the terrestrial atmosphere.

The paper is organized as follows: in Sect. 2, measurements of SSI variations are described, and their accuracy on time scales from days to 11-yr solar cycle is discussed. In Sect. 3 we delineate mechanisms responsible for the SSI variations, outline
10 methods of irradiance reconstructions and briefly describe and compare several of the most broadly used models of SSI variations. Section 4 discusses the impact of the current lower and upper boundaries of SSI solar cycle estimated variations on CCM simulations. A summary and concluding remarks are provided in Sect. 5.

2 Solar irradiance measurements

In this section we present solar irradiance observations. We describe the evolution of measurements carried out from space since 1978 (Sect. 2.1) and discuss major instrumental and measurement problems that limit the creation of single composite time series from existing records. We also present instruments and techniques used to derive four SSI data sets that are employed for CCM simulations, as well as results
15 of the recent re-analysis of SORCE/SIM measurements (Sect. 2.2.1). We then present results of the studies on the absolute values of the TSI and discussion of measurement uncertainties (Sect. 2.3).

Overview:

- Recent observations by SORCE/SIM suggest a larger decrease (by a factor of 2–6) in the UV (200–400 nm) during the declining phase of solar cycle 23, which

25

[Title Page](#)[Abstract](#)[Introduction](#)[Conclusions](#)[References](#)[Tables](#)[Figures](#)[◀](#)[▶](#)[◀](#)[▶](#)[Back](#)[Close](#)[Full Screen / Esc](#)[Printer-friendly Version](#)[Interactive Discussion](#)

lasted from 2003 to 2009, compared to other observations and from prior solar cycles.

- An improved degradation correction that assumes near constant SSI during the very recent solar minimum (2008–2009) leads to a reduction of the UV solar cycle variations observed by SORCE/SIM by about 50 %, still higher than other results.
5
- Satellite measurements show that the mean TSI is lower than the value derived from earlier observations. For many years, the canonical value of the average TSI was $1365.4 \pm 1.3 \text{ W m}^{-2}$ whereas now the most accurate, and generally accepted, value is $1361 \pm 0.5 \text{ W m}^{-2}$.

10 2.1 Introduction

For many centuries, the Sun has been considered as an example of stability and, not surprisingly, the TSI, i.e. the quantity of radiative power density (W m^{-2}) at normal incidence on top of the atmosphere, at a Sun–Earth distance of one astronomical unit, today is still referred to by many as the solar constant. However, regular space-based
15 observations that started in 1978 (Willson et al., 1981) have revealed that the TSI varies over time scales of minutes to decades, and probably even longer (e.g. Fröhlich, 2006, 2009).

The most conspicuous variation of the TSI is a 0.1 % modulation in phase with the solar activity or sunspot cycle. Although quantifying such small variations is a major
20 technological challenge, it is strongly motivated by the desire to understand solar variability, and even more so by the importance of the TSI for terrestrial energy budget studies (Trenberth et al., 2009).

The TSI is the spectral integral of SSI over all wavelengths but its weak variability masks the fact that relative SSI variations show a strong wavelength dependence
25 (Fig. 1). In particular, the visible and NIR bands are the least variable of the solar spectrum with a relative solar cycle amplitude of the same order as for the TSI (0.1 %), whereas values of 1 to 20 % are observed in the UV variations, and in excess of 100 %

[Title Page](#)[Abstract](#)[Introduction](#)[Conclusions](#)[References](#)[Tables](#)[Figures](#)[◀](#)[▶](#)[◀](#)[▶](#)[Back](#)[Close](#)[Full Screen / Esc](#)[Printer-friendly Version](#)[Interactive Discussion](#)

**Spectral irradiance
and climate**

I. Ermolli et al.

[Title Page](#)[Abstract](#)[Introduction](#)[Conclusions](#)[References](#)[Tables](#)[Figures](#)[|◀](#)[▶|](#)[◀](#)[▶](#)[Back](#)[Close](#)[Full Screen / Esc](#)[Printer-friendly Version](#)[Interactive Discussion](#)

in the soft X-ray range (below 10 nm). Each individual spectral band has a markedly different impact on the terrestrial atmosphere.

Regular space-based monitoring of the solar spectrum over a broad range, covering, in addition to the UV, the visible and the IR up to 2.4 µm, started with the launch of ENVISAT/SCIAMACHY in 2002 and SORCE/SIM in 2003. Measurements in the UV below 400 nm began several decades earlier (Fig. 3). Most of these earlier measurements, however, are difficult to use for quantifying the solar variability, for reasons that will be detailed below.

The longest records of SSI measurements were provided by SOLSTICE and SUSIM aboard the UARS (Upper Atmosphere Research Satellite) spacecraft (Rottman et al., 2004). These instruments observed solar UV radiation between 120 and 400 nm from 1991 to 2001 and 2005, respectively. These measurements pointed to the importance of the irradiance variations in the UV (Woods et al., 2000; Rottman et al., 2001; Floyd et al., 2002, 2003), although the solar cycle variability of solar radiation above approximately 250 nm remained relatively uncertain due to insufficient long-term stability of the instruments (Woods et al., 1996). In addition to SOLSTICE and SUSIM, there is the long time series of 200–400 nm solar UV observations by several NOAA SBUV instruments, which had underflight calibrations aboard the Space Shuttle (Cebula et al., 1998).

Regular observations of the visible and NIR bands covering more than one year started with SOHO/VIRGO-SPM (Fröhlich et al., 1997) in 1996 at three selected bands and continued with the ERS/GOME (Weber et al., 1998; Burrows et al., 1999), ENVISAT/SCIAMACHY (Bovensmann et al., 1999), SORCE/SIM (Harder et al., 2005a,b), and ISS/SOLSPEC (Thuillier et al., 2009) instruments. An overview of all SSI measurements from space as a function of the period of observations and wavelength coverage (above 100 nm) is given in Fig. 3. Some SSI missions are described in more detail in Sect. 2.2.

Merging all UV observations into a single homogeneous composite record is a major challenge (Deland et al., 2004) that is hampered by several problems. First, the

lifetime of most instruments does not exceed a decade. This makes long-term observations covering periods that exceed single instrument lifetimes, of prime interest for climate models, very difficult. A second obstacle is the differing technologies and modes of operation of various space-based instruments. The cross-calibration of individual records is further hampered by the fact that overlapping observations disagree (see Sect. 2.2.4), and the existing data records are spectrally and temporally intermittent. Although missing observations can be filled in by using data regression based on time series of solar proxies such as the Mg II index, which are well correlated with UV variations (Deland and Cebula, 1993; Viereck et al., 2001; Lean, 1997), none of the existing solar proxies can properly reproduce solar irradiance in a spectral band on all time scales (Dudok de Wit et al., 2009).

The most critical issue for all SSI instruments is the optical degradation caused by the energetic radiation in the space environment. Two options have been employed to account for instrumental degradations. The first one is to provide redundancy in the instrument design, by using, e.g. a dual spectrometer setup with detectors that experience different accumulated exposure time or by planning redundancies in spectral channels and calibration lamps from which degradation corrections can be derived. This approach was used, for instance, for UARS/SUSIM and SORCE/SIM (Brueckner et al., 1993; Harder et al., 2005a). The second option is to use stable external calibration targets like selected stars, as is done for UARS/SOLSTICE and SORCE/SOLSTICE (McClintock et al., 2005). Sensitivity changes and degradation are strongly wavelength-dependent, which makes creating a properly cross-calibrated SSI record very difficult. One attempt for a composite SSI time series in the UV is provided by DeLand and Cebula (2008).

Cross-calibration of different SSI records is also limited by the lack of realistic confidence intervals for the existing data. This aspect has been thoroughly investigated for the TSI (see Sect. 2.3) and sound estimates have been obtained for time scales from days to years. No meaningful estimates, however, exist for time scales exceeding one decade, which are needed for climate studies. The situation is much worse for SSI

[Title Page](#)[Abstract](#)[Introduction](#)[Conclusions](#)[References](#)[Tables](#)[Figures](#)[|◀](#)[▶|](#)[◀](#)[▶](#)[Back](#)[Close](#)[Full Screen / Esc](#)[Printer-friendly Version](#)[Interactive Discussion](#)

measurements, whose relative uncertainties often are two to three orders of magnitude larger.

In the following subsections a brief summary of recent SSI observations is given. Also a brief description of recent developments regarding the absolute values of the
5 TSI, and its variability is provided.

2.2 SSI time series

2.2.1 SCIAMACHY and GOME

SCIAMACHY (SCanning Imaging Absorption spectroMeter for Atmospheric CHartographY) and GOME (Global Ozone Monitoring Experiment) onboard the ENVISAT and

10 ERS-2 satellites, respectively, are atmospheric sounders that measure terrestrial atmospheric trace gases (Burrows et al., 1999; Bovensmann et al., 1999; Bovensmann et al., 2011). The primary purpose of direct solar measurements by SCIAMACHY and the two GOMEs (a second GOME is flying since 2006 on METOP-A) is to Sun-normalise the backscattered light from the terrestrial atmosphere, which is then inverted to determine atmospheric trace gas amounts. This normalisation does not require absolute radiometric calibration and cancels out degradation effects. The SCIAMACHY and GOME instruments have been radiometrically calibrated before launch.
15

In order to provide estimates for solar cycle variability from SCIAMACHY measurements (230 nm–2.4 μm) without the need for a detailed degradation correction, the
20 SCIAMACHY proxy model was developed by fitting solar proxy time series to observed SCIAMACHY measurements over several 27-day solar rotation periods (Pagaran et al., 2009). The proxies used in this model are the photometric sunspot index (Balmaceda et al., 2009) and the Mg II index (Weber et al., 2013) for sunspot darkening and facular brightening. Assuming that the fitting parameters linearly scale from solar rotations to an 11-yr solar cycle, one can then use the solar proxies to extrapolate beyond the lifetime of the single instrument (Pagaran et al., 2011b). Note, however, that this
25 assumption might not be accurate, and probably results in an underestimate of the

[Title Page](#)[Abstract](#)[Introduction](#)[Conclusions](#)[References](#)[Tables](#)[Figures](#)[◀](#)[▶](#)[◀](#)[▶](#)[Back](#)[Close](#)[Full Screen / Esc](#)[Printer-friendly Version](#)[Interactive Discussion](#)

**Spectral irradiance
and climate**

I. Ermolli et al.

[Title Page](#)[Abstract](#)[Introduction](#)[Conclusions](#)[References](#)[Tables](#)[Figures](#)[◀](#)[▶](#)[◀](#)[▶](#)[Back](#)[Close](#)[Full Screen / Esc](#)[Printer-friendly Version](#)[Interactive Discussion](#)

phase of cycle 23 by a factor of 3–10 depending on wavelength (Deland and Cebula, 2012; Figs. 2, 4, and 8).

These discrepancies with prior cycle observations and with models have inspired new efforts to better understand the sources of instrument degradation that might have affected SORCE instruments and previous instruments as well. A workshop was held in February 2012 at the National Institute for Standards and Technology (NIST) to understand causes of instrument degradation. The meeting concentrated on SSI instrument observations, capabilities, and estimated spectral irradiance uncertainties, methods of correcting for degradation, and refining estimated uncertainties. All detectors and optics suffer some degradation in space, largely due to exposure to solar light and also due to hydrocarbon contamination that dominates below 400 nm. New models of degradation based on total dose, rather than just exposure time, are now being developed for the SORCE instruments. In addition to using physical degradation models, degradation trends can be analyzed by considering the expected invariance of SSI over the solar cycle minimum. This method has been developed by Woods (2012) and applied to data over the last solar cycle minimum (2008–2009) to derive plausible degradation trends for SORCE/SIM and SORCE/SOLSTICE. This method identifies near-identical solar activity levels on both sides of the minimum to extract the functional dependence of the deviation from invariance over the solar minimum. This analysis showed relative agreement for all instruments and models for the solar cycle variability from 30 nm to 300 nm for solar cycles 21 through 24. For the 300 nm to 400 nm range, SORCE/SIM indicates about five times more variability than the UARS/SOLSTICE measurements and most model (see Sect. 3.3) results. The integrated UV irradiance from 200 nm to 400 nm, relative to the measured TSI change (Fig. 2), dropped from 190 % with the original SORCE/SIM analysis (Harder et al., 2009) to 110 % (Woods, 2012). This still requires compensation from out-of-phase trends in other spectral bands in wavelengths longer than 400 nm. Other analyses of solar cycle variability suggests that the UV variability in the 200 nm to 400 nm range is about 60 % of the measured TSI change (Krivova et al., 2006; Pagaran et al., 2009; Morrill et al., 2011b, see Sect. 3).

Spectral irradiance and climate

I. Ermolli et al.

[Title Page](#)

[Abstract](#)

[Introduction](#)

[Conclusions](#)

[References](#)

[Tables](#)

[Figures](#)

[◀](#)

[▶](#)

[◀](#)

[▶](#)

[Back](#)

[Close](#)

[Full Screen / Esc](#)

[Printer-friendly Version](#)

[Interactive Discussion](#)



While the re-analysis of SORCE data may resolve some of these differences, to improve our understanding of SSI variability new and improved, upgraded observations of the SSI are required. The next generation SIM instrument has been built for the NOAA/NASA Total Solar Irradiance Sensor (TSIS) mission and includes many design improvements for reducing noise and improving in-flight degradation tracking. The TSIS SIM is currently undergoing laboratory calibrations at LASP using radiometric calibration technology similar to that employed in LASP's TSI Radiometric Facility (TRF) that helped to resolve the source of offsets among various TSI instruments (Kopp and Lean, 2011); see also Sect. 2.3. The TSIS mission might be launched in 2016, but it is highly unlikely that TSIS/SIM and SORCE/SIM observations will overlap in time due to the expected lifetime of the SORCE batteries.

2.2.3 SOLSPEC

The SOLar SPECtrum instrument (SOLSPEC; Thuillier et al., 2009) is composed of three double monochromators (170–390 nm, 380–850 nm, 800–3000 nm) and a set of lamps allowing corrections for aging related to the harsh space environment. The SOLSPEC spectrometer flew several times on the Space Shuttle and its twin instrument, SOSP (SOlar SPectrum), was placed on the EURECA (EUropean Retrieval Carrier) platform for 10 months (April 1993 to January 1994). These missions have provided data to build the ATLAS (ATmospheric Laboratory for Applications and Science) spectra, specifically ATLAS-1 (March 1992) and ATLAS-3 (November 1994) (Thuillier et al., 2004), which are composites using UARS/SUSIM and UAR/SOLSTICE data from Lyman- α at 121 nm to 200 nm, and ATLAS/SSBUV, ATLAS/SUSIM, and ATLAS/SOLSPEC from 200 to 400 nm, ATLAS/SOLSPEC from 400 to 850 nm, and EURECA/SOSP from 800 to 2400 nm. The ATLAS spectra were calibrated to absolute radiometric scale using the blackbody of the Heidelberg Observatory, and tungsten and deuterium lamps calibrated by NIST.

SOLSPEC has been up-graded for operations onboard the International Space Station (ISS) by implementing several changes in the electronics, optics, and mechanisms

[Title Page](#)[Abstract](#)[Introduction](#)[Conclusions](#)[References](#)[Tables](#)[Figures](#)[◀](#)[▶](#)[◀](#)[▶](#)[Back](#)[Close](#)[Full Screen / Esc](#)[Printer-friendly Version](#)[Interactive Discussion](#)

and by adding redundant components in order to generate data with proper degradation correction. ISS/SOLSPEC has been calibrated to an absolute scale at the Physikalisch-Technische Bundesanstalt (PTB) using the BB3200pg blackbody radiator (Sperfeld et al., 1998). Over the whole spectral range, SOLSPEC accuracy is within 5 2 to 3 %. The SOLSPEC spectrometer has been in operation since February 2008 onboard the ISS along with the SOL-ACES (SOLar Auto-Calibrating EUV/UV Spectrophotometers) instrument measuring below 150 nm. When the ISS orientation allows, ISS/SOLSPEC records the solar spectral irradiance. Presently, data have been obtained during the solar minimum preceding solar cycle 24 and at some specific periods 10 during its rising phase for direct comparisons with SORCE/SIM observations (Thuillier et al., 2012).

2.2.4 Statistical analysis of SSI time series

As mentioned in Sect. 2.1, the assessment of long-term variations in SSI observations can be done only by stitching together different records that, individually, often 15 do not last for more than a few years and are almost always offset by different calibration scales. The first systematic effort toward building such a single composite data set for the UV was done by DeLand and Cebula (2008), who created a data set with daily spectra covering the wavelength range 120–400 nm for the time period November 1978 to August 2005. However, the instruments frequently differed in their radiometric 20 calibration and in their long-term stability. One is therefore left with making subjective adjustments that can dramatically alter the interpretation of long-term variations (Lockwood, 2011) and, for example, mimic a solar cycle variation that does not exist. A more objective approach consists of incorporating these instrumental discrepancies in the reconstruction, and then explicitly using them as a contribution to the overall uncertainty. 25 A Bayesian statistical framework is ideal for this analysis.

To illustrate this approach, we concentrate on the solar cycle (i.e. decadal) modulation, which has the advantage of being one of the conspicuous signatures of solar

[Title Page](#)[Abstract](#)[Introduction](#)[Conclusions](#)[References](#)[Tables](#)[Figures](#)[◀](#)[▶](#)[◀](#)[▶](#)[Back](#)[Close](#)[Full Screen / Esc](#)[Printer-friendly Version](#)[Interactive Discussion](#)

variability in climate records while offering sensitive means for diagnosing the quality of the solar observations.

Our analysis consists of comparing the 11-yr modulation amplitude and phase for each solar instrument separately and identifying possible changes since 1978. One can reasonably assume that the modulation phase and amplitude of SSI are unlikely to undergo major changes from one solar cycle to another because all other solar proxies (Mg II index, f10.7 solar flux) change over multiple solar cycles. We estimate the modulation amplitude and phase by running an 11-yr running mean through the data. The phase reference is given by the Mg II core-to-wing ratio, which is the most widely used proxy for the solar UV (Viereck et al., 2001).

The modulation phase and amplitude can be accurately estimated only if the observations span at least one solar cycle, which is rarely the case. An important step thus consists in extrapolating each set of observations backward and forward in time while preserving its statistical properties with respect to all other observations (cross-correlation, etc.). This is made possible thanks to the empirical evidence for all neighboring spectral bands to evolve remarkably coherently in time, on time scales of hours and beyond (Lean et al., 1982; Amblard et al., 2008). This coherency, which is rooted in the strong magnetic coupling between solar atmospheric layers, allows us to describe all salient features of the variability in the SSI with just a few degrees of freedom, typically three in the UV. The appropriate approach is based on the expectation-maximisation technique (Dudok de Wit, 2011). The result is that for each wavelength there are as many records as there are instruments observing that wavelength. The overall dispersion of the various observations is then naturally reflected by the dispersion of the reconstructions, and so no offset or trend adjustments are required.

Figure 4 illustrates the extrapolation for the 220–240 nm band, which is important for ozone production (e.g. Rozanov et al., 2002). This example shows that all observations vary in phase with the solar cycle but differ considerably in their modulation amplitude. The observations from SORCE exhibit a larger modulation amplitude, as already mentioned above.

Spectral irradiance and climate

I. Ermolli et al.

[Title Page](#)

[Abstract](#)

[Introduction](#)

[Conclusions](#)

[References](#)

[Tables](#)

[Figures](#)

[◀](#)

[▶](#)

[◀](#)

[▶](#)

[Back](#)

[Close](#)

[Full Screen / Esc](#)

[Printer-friendly Version](#)

[Interactive Discussion](#)



Because this approach provides as many UV composites as there are observations, we can test whether the observations from SORCE/SIM and SORCE/SOLSTICE are compatible with those from other instruments, most of which were obtained during preceding solar cycles. The comparison is summarized in Fig. 5, which compares the modulation amplitude and phase of SORCE versus the distribution obtained by the other instruments. We conclude that all instruments agree remarkably well below 200 nm; at longer UV wavelengths, the modulation amplitude inferred from SORCE/SOLSTICE is systematically larger by a factor of two to six at all wavelengths. The simultaneous sharp drop in its phase raises doubts about the consistency of the observations from SORCE. Assuming that there is no reason for the SSI to be unusual during the last solar cycle only, we conclude that these observations are likely to be affected by instrumental drifts, in agreement with the conclusions from Lean and DeLand (2012). This may also be the case for SORCE/SIM between 308 and 340 nm, although the departure from other observations is much less significant here.

2.3 Total solar irradiance (TSI) time series

Some CCM simulation still assume a SSI variability that is derived from TSI time series (see Sect. 4), thereby fixing the relative spectral contribution to TSI variability. In addition, TSI time series also provide constraints for empirical and semi-empirical models of SSI variations (see Sect. 3). For many years, the canonical value of the average TSI was $1365.4 \pm 1.3 \text{ W m}^{-2}$. Now, the most accurate, and generally accepted, value is $1361 \pm 0.5 \text{ W m}^{-2}$ (Kopp and Lean, 2011; Schmutz et al., 2012). This lower value will be used in the data assimilation and meteorological re-analysis project like ERA-CLIM at ECMWF (D. Dee, ECMWF, personal communication 2012, and see <http://www.era-clim.eu/>).

TSI variability was already predicted in the 1920s from ground-based observations (Abbot et al., 1923). Accurate measurement of TSI and detection of its variability requires observations from space. The first report of the variable solar irradiance with correct amplitudes was made by Hickey et al. (1980). Later observations differed markedly

[Title Page](#)[Abstract](#)[Introduction](#)[Conclusions](#)[References](#)[Tables](#)[Figures](#)[◀](#)[▶](#)[◀](#)[▶](#)[Back](#)[Close](#)[Full Screen / Esc](#)[Printer-friendly Version](#)[Interactive Discussion](#)

in their absolute values but all basically agreed in the relative amplitude of the TSI variations. In Table 1 we list the main space experiments that have measured TSI, together with their observed variabilities. The given numbers are biased by the duration of the experiments and their phase relative to the solar cycle, but the overall result is that TSI variations are observed to be on the order of about 0.5 % standard deviation from the mean value.

Lee et al. (1995) estimate the absolute accuracy of the NIMBUS7/HF instrument to be 0.5 % and that of ERBS/ERBE 0.2 %. Willson (1979) expected his SMM/ACRIM-I experiment to remain within 0.1 % for at least a year. Fröhlich and Lean (1998) state that the absolute measurements of the early radiometers are uncertain to about 0.4 %, which corresponds to 5.5 W m^{-2} . The main reason for this relatively large spread was due to the uncertainty in the aperture area. When the technology for determining aperture area improved the agreements among the measurements improved. However, the SORCE/TIM experiment proved to be a new outlier. Lawrence et al. (2003) claim an uncertainty of 0.5 W m^{-2} , i.e. accurate to 350 ppm. Because SORCE/TIM is 4.5 and 5 W m^{-2} below SOHO/VIRGO and ACRIM/ACRIM-III, the uncertainties given by the instrument teams do not overlap (Kopp and Lean, 2011).

The PREMOS experiment on the French satellite PICARD, which was launched in July 2010, has solved this discrepancy. The radiometers of the PICARD/PREMOS experiment have been calibrated in two different and independent ways. The first is a calibration in power response as reported by Schmutz et al. (2009). In addition, the TSI radiometer of PICARD/PREMOS is, so far, the first space instrument that has been calibrated in irradiance in vacuum. This was done at the Total solar irradiance Radiometer Facility (TRF) located at the Laboratory for Atmospheric and Space Physics (LASP) in Boulder, Colorado, USA (Fehlmann et al., 2012). The irradiance calibration is accurate to 330 ppm. PICARD/PREMOS agrees with SORCE/TIM to within 0.4 W m^{-2} , with PICARD/PREMOS being lower (Schmutz et al., 2012). Thus, the new experiments are now well within their common uncertainty range and the uncertainty difference between independent measurements of the solar constant has decreased by a factor of ten.

Spectral irradiance and climate

I. Ermolli et al.

[Title Page](#)[Abstract](#)[Introduction](#)[Conclusions](#)[References](#)[Tables](#)[Figures](#)[◀](#)[▶](#)[◀](#)[▶](#)[Back](#)[Close](#)[Full Screen / Esc](#)[Printer-friendly Version](#)[Interactive Discussion](#)

The characterisation of the SORCE/TIM, ACRIM/ACRIM III, and SOHO/VIRGO witness units at TRF, and the calibration of PICARD/PREMOS, resolved the source of the discrepancy among TSI observations (Kopp and Lean, 2011; Schmutz et al., 2012). Instruments such as PMO6 and ACRIM type having a view-limiting aperture in front

- 5 and a smaller precision aperture that defines the irradiance area have a large amount of scattered light within the instrument. This additional light is not fully absorbed by the baffle system and produces scattered light contributing to extra power measured by the cavity. Scattered light was one of the potential systematic errors suspected by Butler et al. (2008). Subsequent ground testing involving the different instrument teams
10 verified scattering as the primary cause of the discrepancy between the TIM measurements and the erroneously high values of other TSI instruments. New stray light corrections have been assigned to ACRIM/ACRIM-III (based on spare instruments) and its stray light contribution is indeed of the order as the observed differences. For SOHO/VIRGO the scattered light issue was not the reason for its discrepant reading.
15 VIRGO is traceable to the World Radiometric Reference (WRR) but recently, new comparisons have revealed that the WRR has a systematic offset (Fehlmann et al., 2012). The WRR offset produced approximately the same systematic shift as the scattering error. Thus, in summary, there is now a consistent evaluation of the solar constant from four instruments: SORCE/TIM, SOHO/VIRGO (corrected), ACRIM/ACRIM-III (corrected), and from PICARD/PREMOS.

- 20 TSI changes can be measured to much higher precision than absolute TSI values. On short time scales, relative measurements are accurate to a few ppm on a daily average. On longer time scales of years and tens of years, the stability of the measurements are much more difficult to evaluate. Claims of stabilities of less than 100 ppm over ten years (Fröhlich, 2009) are most likely too optimistic. A more realistic estimate comes from comparing independent composites that have been constructed. Over the time of the last solar cycle these agree to within about 0.2 W m^{-2} or about 20 ppm yr^{-1} . For pre-1996 measurements even higher uncertainties for the systematic drifts have to

Spectral irradiance and climate

I. Ermolli et al.

[Title Page](#)

[Abstract](#)

[Introduction](#)

[Conclusions](#)

[References](#)

[Tables](#)

[Figures](#)

[◀](#)

[▶](#)

[◀](#)

[▶](#)

[Back](#)

[Close](#)

[Full Screen / Esc](#)

[Printer-friendly Version](#)

[Interactive Discussion](#)



be adopted. Despite these conservative assessments, TSI time record is a factor of ten more accurate than any SSI observation.

2.4 Concluding remarks

Even though the large UV solar cycle variations indicated by SIM/SORCE observations (Harder et al., 2009) may be smaller by half based upon new calibration corrections, other observations and statistical analysis of existing long-term satellite time series still show some inconsistencies in the derived SSI solar cycle variability. The main reason for this are uncertainties in the long-term stability of space observations due to degradation issues related to the hard radiation environment in space. There is certainly a need for additional and continuous SSI observations in the coming years.

In general, the precision of SSI measurements is quite high on solar rotational timescales; however, very little is known about stability estimates over extended periods of time that are relevant for climate, from a few years, to decades and longer.

With the aging SORCE mission, a gap in long-term observations from space instruments with a primary focus on SSI measurements is likely to occur. Nevertheless several satellite missions that are more dedicated to the observation of the Earth's atmosphere will continue to provide information on part of the SSI spectra.

3 Models of SSI variations

This section discusses models of SSI variations. We give the motivation for models in Sect. 3.1. In Sect. 3.2, we discuss the mechanisms responsible for the irradiance variations, with special emphasis on the possible differences in the spectral response of the irradiance to the modulating agents. We then (Sect. 3.3) describe the basic principles and key components of the models and review five current SSI models that are used as input to climate studies. Finally, in Sect. 3.4, we compare the models to

[Title Page](#)

[Abstract](#)

[Introduction](#)

[Conclusions](#)

[References](#)

[Tables](#)

[Figures](#)

[◀](#)

[▶](#)

[◀](#)

[▶](#)

[Back](#)

[Close](#)

[Full Screen / Esc](#)

[Printer-friendly Version](#)

[Interactive Discussion](#)



each other, confront them with the available observational data and summarize the findings of this section.

Overview:

- There has been steady progress in modelling solar spectral irradiance variations, and a number of models are now available that can be used as input for climate studies.
- The main uncertainty in the models concerns the wavelength range 220–400 nm, where the magnitude of the variations differs by as much as a factor of three between models (Fig. 2).
- Although large, this uncertainty is still significantly smaller than the discrepancy in this range (as much as a factor of 6) between models and the SORCE/SOLSTICE and SORCE/SIM measurements over the declining phase of cycle 23.
- The agreement of the models with the earlier measurements in the UV (e.g. by UARS/SOLSTICE and UARS/SUSIM) is significantly better than that with the SORCE data.
- The out-of-phase variability in the visible, at 400–700 nm, observed by SORCE/SIM is not reproduced by the models (except in the SRPM model, where this is by design, however).
- Semi-empirical models of the solar atmospheric structure have not yet been tested at all wavelengths and can, in principle, be tuned to better match SORCE SSI data. It will be very difficult, however, to reconcile these models with other available SSI observation or TSI data.

[Title Page](#)

[Abstract](#)

[Introduction](#)

[Conclusions](#)

[References](#)

[Tables](#)

[Figures](#)

[◀](#)

[▶](#)

[◀](#)

[▶](#)

[Back](#)

[Close](#)

[Full Screen / Esc](#)

[Printer-friendly Version](#)

[Interactive Discussion](#)



3.1 Introduction

As described in Sect. 2, measurements of solar irradiance from space started in 1978. Whereas the TSI has been monitored regularly, data for the spectral irradiance are more disrupted. Since degradation and sensitivity changes vary strongly with wave-lengths and from one instrument to another (e.g. DeLand and Cebula, 2008), a proper self-consistent cross-calibration of different observational sets is a major challenge. The recent measurements by SORCE complicate the situation further. Longer, uninterrupted, more stable and reliable observational time series are critical for understanding the origin of the differences between SSI measurements and improving our knowledge of SSI variations. However, the physics of the underlying processes also needs to be understood better, in order to facilitate the construction of more realistic models of SSI variations. Such models are particularly crucial since climate studies including stratospheric chemistry urgently need long and reliable SSI data sets for realistic simulations. Acquiring sufficiently long SSI time series is a long process and making them more reliable requires flying multiple new instruments, which will not happen for some time. Even when such time series do become available, they can only be extended into the past or future with the help of suitable models.

Although considerable progress has been made in modeling the TSI variability (e.g. Foukal and Lean, 1990; Chapman et al., 1996; Fröhlich and Lean, 1997; Fligge et al., 2000; Preminger et al., 2002; Ermolli et al., 2003; Krivova et al., 2003; Wenzler et al., 2004, 2005, 2006; Ball et al., 2012), modelling the SSI is more tricky, leaving considerable room for improvement. Here we describe recent progress in SSI modelling, briefly review five widely used SSI models (NRLSSI, SATIRE-S, COSI, SRPM and OAR) and discuss remaining uncertainties and open issues.

25 3.2 Mechanisms of irradiance variations

Although various mechanisms have been proposed to explain the variation of solar irradiance, it is now accepted that observed variations in TSI (i.e. over the last 3.5

Spectral irradiance and climate

I. Ermolli et al.

[Title Page](#)

[Abstract](#)

[Introduction](#)

[Conclusions](#)

[References](#)

[Tables](#)

[Figures](#)

[◀](#)

[▶](#)

[◀](#)

[▶](#)

[Back](#)

[Close](#)

[Full Screen / Esc](#)

[Printer-friendly Version](#)

[Interactive Discussion](#)



solar cycles) are predominantly caused by magnetic features on the solar surface. We cannot rule out that on longer time scales other mechanisms play a significant role, but this is beyond the scope of this paper.

Empirically it has been known for a long time that magnetic features on the solar surface are generally either dark (sunspots, pores) or bright (magnetic elements forming faculae and the network) when averaged over the solar disk. Two questions arise from this observation: why are some flux tubes (the theoretical concept used to describe faculae and sunspots) bright, while others are dark? What happens to the energy flux blocked by sunspots (or equivalently, where does the excess energy emitted by faculae come from)?

The strong magnetic field within both small and large magnetic flux tubes reduces the convective energy flux. The vertical radiative energy flux in the convection zone is comparatively small and cannot compensate a reduction in convective flux. This leads to a cooling of magnetic features.

The magnetic features are evacuated due to the large internal magnetic pressure and horizontal balance of total (i.e. gas plus magnetic) pressure. Hence, these evacuated magnetic structures are also heated by radiation flowing in from their dense and generally hot walls. This radiation efficiently heats features narrower than roughly 250 km, making them brighter than the mainly field-free part of the photosphere, especially when seen near the limb where the bright walls are best visible (Spruit, 1976; Keller et al., 2004). For larger features, the radiation does not penetrate most of their volume (the horizontal photon mean free path is roughly 50–100 km), so that features greater than roughly 400 km in diameter remain dark (pores and sunspots); cf. Grossmann-Doerth et al. (1994).

What happens with the energy that gets blocked by sunspots? According to Spruit (1982), this energy gets redistributed throughout the convection zone and is re-emitted again slowly over its Kelvin-Helmholtz timescale, which exceeds the lifetime of sunspots by orders of magnitude. Similarly, the excess radiation coming from small flux tubes (which act as leaks in the solar surface, since these evacuated features

[Title Page](#)[Abstract](#)[Introduction](#)[Conclusions](#)[References](#)[Tables](#)[Figures](#)[◀](#)[▶](#)[◀](#)[▶](#)[Back](#)[Close](#)[Full Screen / Esc](#)[Printer-friendly Version](#)[Interactive Discussion](#)

**Spectral irradiance
and climate**

I. Ermolli et al.

[Title Page](#)[Abstract](#)[Introduction](#)[Conclusions](#)[References](#)[Tables](#)[Figures](#)[◀](#)[▶](#)[◀](#)[▶](#)[Back](#)[Close](#)[Full Screen / Esc](#)[Printer-friendly Version](#)[Interactive Discussion](#)

an effect. But pores are relatively short lived and too few in number. Hence, any long-lasting global dimming in the visible at times of high activity, can only be produced by the small magnetic elements, specifically those in the network (these are much more numerous and more evenly distributed). However, such small-scale magnetic elements
5 are unlikely candidates to produce a decrease in the visible irradiance along with increased UV irradiance. Firstly, magnetic elements in the network are bright even in the continuum and at disk centre (e.g. Kobel et al., 2011). Secondly, Röhrbein et al. (2011) have shown that the darker than average appearance of some magnetic elements is largely due to spatial smearing of the observations (although there may be some darkening due to the inhibition of convection around magnetic features). Thirdly, there are
10 also many spectral lines in the visible, which brighten significantly in magnetic elements and counteract any darkening in the continuum. Finally and most importantly, magnetic elements near the limb are always rather bright, so that averaged over the solar disk small-scale magnetic features are expected to lead to a brightening.

15 This implies that the measurements by SORCE/SIM of a change in the irradiance at visible wavelengths out-of-phase with TSI (Harder et al., 2009) are not compatible with a magnetic field as the source of the SSI variations in the visible. However, the SSI variations in the visible are an important contributor to TSI variations (see Fig. 2) and the above incompatibility would be strongly contradicted by the result of Ball et al.
20 (2012) that 92 % of TSI variations are reproduced by the evolution of the magnetic field at the solar surface.

3.3 Models

It was noticed soon after the beginning of routine monitoring of TSI from space, that changes in TSI were closely related to the evolution of different brightness structures
25 on the visible solar disc (Foukal and Vernazza, 1979; Willson et al., 1981; Oster et al., 1982; Eddy et al., 1982; Foukal and Lean, 1986). These brightness structures (such as sunspots, pores, faculae, plage and network) are manifestations of the solar magnetic field emerging at the Sun's surface (see Sect. 3.2). Thus their evolution in a global

[Title Page](#)[Abstract](#)[Introduction](#)[Conclusions](#)[References](#)[Tables](#)[Figures](#)[|◀](#)[▶|](#)[◀](#)[▶](#)[Back](#)[Close](#)[Full Screen / Esc](#)[Printer-friendly Version](#)[Interactive Discussion](#)

sense (and without looking too closely at the details of the temporal evolution) can be relatively well represented by different, typically disc-integrated, proxies of solar magnetic activity, such as the sunspot number or area, plage area, the solar radio flux at 10.7 cm (f10.7), the Mg II core-to-wing index, or the Ca II K line. This has widely been used in the oldest (but still widely deployed) irradiance models (e.g. Donnelly et al., 1982; Foukal and Lean, 1990; Chapman et al., 1996, 2012; Fröhlich and Lean, 1997; Fligge et al., 1998; Lean, 2000; Preminger et al., 2002; Jain and Hasan, 2004; Pagaran et al., 2009). In these models, the measured irradiance variations are fitted via a set of activity proxies through multiple regressions.

The success and the limitations of the regression methods in accounting for measured TSI variations (on time-scales of days to years) gave a strong impetus to the development of more sophisticated and physics-based models. Such models consider contributions of different brightness structures to the irradiance change separately. Thus the solar energy output is the sum of the fluxes emerging from all the features observed on the solar visible surface (corresponding to the solar photosphere); the number and type of disk features accounted for depends on the model. Usually these models require two prime ingredients: (1) the surface area covered by each photospheric component as a function of time, and (2) the brightness of each component as a function of wavelength and often also of the position on the solar disc.

(1) The surface area coverage by each photospheric component (i.e. sunspot umbrae and penumbrae, pores, faculae, plage, network etc.) is derived from observations. These could be disc-integrated data (e.g. sunspot number, sunspot area, facular or plage area, Mg II index, cosmogenic isotope data etc.; Fligge et al., 1998; Solanki and Unruh, 1998; Fligge and Solanki, 2000; Krivova et al., 2007, 2010; Shapiro et al., 2011; Vieira et al., 2011) or spatially resolved observations (Fligge et al., 2000; Ermolli et al., 2003; Krivova et al., 2003; Fontenla et al., 2004, 2011; Fontenla and Harder, 2005; Wenzler et al., 2004, 2005, 2006; Unruh et al., 2008; Ball et al., 2011, 2012).

(2) The brightness of individual photospheric components is calculated using various radiative transfer codes, such as SRPM (Fontenla et al., 1999, 2011), ATLAS9

[Title Page](#)

[Abstract](#)

[Introduction](#)

[Conclusions](#)

[References](#)

[Tables](#)

[Figures](#)

[◀](#)

[▶](#)

[◀](#)

[▶](#)

[Back](#)

[Close](#)

[Full Screen / Esc](#)

[Printer-friendly Version](#)

[Interactive Discussion](#)



in SATIRE (Kurucz, 1993) or COSI (Shapiro et al., 2010), from semi-empirical models of the solar atmospheric structure. Such computations are significantly complicated by the departures from the local thermodynamical equilibrium (LTE) conditions (Sect. 2.6 of Rutten, 2003) in the solar atmosphere, as well as by the temporal and spatial bifurcations of the temperature and density in the solar atmosphere (cf. Carlsson and Stein, 1997; Uitenbroek and Criscuoli, 2011). High resolution 3-D models (e.g. Socas-Navarro, 2011) and 3-D MHD simulations (e.g. Vögler, 2005) of the solar atmosphere are gradually becoming available. However, current models cannot yet reproduce available observations over the entire spectrum (Afram et al., 2011). Thus, at present semi-empirical 1-D models of the solar atmosphere are a de-facto standard for calculating irradiance variations. Although these models do not account for the spatial structure and temporal variability of the solar atmosphere, they can be easily adjusted to calculate the solar spectrum and its variability with high accuracy (cf. Fontenla et al., 1999; Unruh et al., 1999). These models do not necessarily catch the average properties of the inhomogeneous solar atmosphere (Loukitcheva et al., 2004; Uitenbroek and Criscuoli, 2011), but, if validated and constrained by the available measurements, they can be considered as a reliable and convenient semi-empirical tool for modelling SSI variability.

Presently, a wide range of solar atmospheric models with different degrees of complexity is available (e.g. Kurucz, 1993; Fontenla et al., 1999, 2009, 2011; Unruh et al., 1999; Penza et al., 2004; Uitenbroek, 2001; Kurucz, 2005; Avrett and Loeser, 2008; Shapiro et al., 2010), most of which go back to Vernazza et al. (1981).

The spectra of the quiet Sun calculated with three different models are shown in Fig. 6 (top panel). All plotted spectra are in reasonable agreement with each other, though models used in COSI and SATIRE are a bit closer to each other than to SRPM. The bottom panel of Fig. 6 shows the flux differences (i.e. the contrasts) between bright active components and the quiet Sun calculated with different models. The calculations were done assuming that the active regions cover the entire solar disk. To calculate the variability, the contrasts have to be weighted by the filling factors (surface area

Spectral irradiance and climate

I. Ermolli et al.

[Title Page](#)

[Abstract](#)

[Introduction](#)

[Conclusions](#)

[References](#)

[Tables](#)

[Figures](#)

[◀](#)

[▶](#)

[◀](#)

[▶](#)

[Back](#)

[Close](#)

[Full Screen / Esc](#)

[Printer-friendly Version](#)

[Interactive Discussion](#)



coverage), which are specific for every model. Thus, different magnitudes of the contrasts do not necessarily imply that the models produce different variability. At the same time, the spectral profile of the contrasts determines the dependence of the variability on the wavelength. While spectral contrasts calculated with SATIRE and COSI are very similar, the SRPM model predicts a very strong decrease of the contrasts in the visible and even yields negative contrasts at some wavelengths. This is not very surprising, however, since the SRPM models shown in Fig. 6 are the most recent versions of the Fontenla et al. (1999) model family that were tuned by Fontenla et al. (2011) to better match SORCE/SIM measurements in the UV and visible (see the description of the SRPM model later in this section).

The advantage of employing radiances computed from the semi-empirical model atmospheres is that they allow computations of solar irradiance at different wavelength (i.e. spectral irradiance). This is not straightforward with the regression models, since in this case the regression coefficients need to be estimated from observations or alternatively, irradiance changes at individual wavelengths need to be somehow scaled from the TSI changes or changes in the irradiance at some other (known) wavelength. This latter technique is also partly used by the SATIRE and NRLSSI models (see below) in the UV (Lean et al., 1997; Lean, 2000; Krivova et al., 2006, 2009).

3.3.1 NRLSSI

The Naval Research Laboratory Solar Spectral Irradiance² (NRLSSI; Lean et al., 1997; Lean, 2000) uses the photospheric sunspot index derived from sunspot area records to describe the evolution of sunspots in time, and Mg II, CaII and f10.7 disk-integrated indices to represent facular brightening.

Below 400 nm, the spectral irradiances are derived from UARS/SOLSTICE observations through a multiple regression analysis with respect to a (SOLSTICE) reference spectrum. The regression analysis includes a facular brightening and a sunspot

²<http://lasp.colorado.edu/lisird/nrlssi/>

blocking component (see Lean et al., 1997; Lean, 2000 for more detail). It is known that the long-term stability of the UARS spectral instruments (both SOLSTICE and SUSIM) was not sufficient to trace solar cycle variability above roughly 220 nm (Woods et al., 1996). Therefore the coefficients are derived from the rotational variability so as to avoid any long-term instrumental effects. This approach thus assumes that spectral irradiance changes show the same linear scaling with a given proxy on rotational as well as cyclical time scales.

Above 400 nm, the facular and sunspot contrasts are largely based on the contrasts presented in Solanki and Unruh (1998). They have been scaled to ensure that the overall (wavelength-integrated) solar cycle change due to sunspots (viz faculae) agrees with the bolometric value for the sunspot blocking (viz facular brightening) derived from TSI modelling (see, e.g. Fröhlich and Lean, 2004).

The quiet-Sun spectrum in NRLSSI is effectively a composite of UARS/SOLSTICE observations (below 400 nm), SOLSPEC (Thuillier et al., 1998) and the model by Kuručz (1991). This composite has been scaled so that its integrated flux corresponds to a TSI value of 1365.5 W m^{-2} .

The employment of UARS/SOLSTICE data up to 400 nm and the use of rotational variability only might be the reasons why the NRLSSI model shows lower variability between 250 and 400 nm compared to other models (see Figs. 2 and 7). Below 250 nm (Figs. 7 and 8) and in the visible at 400–700 nm (Figs. 2 and 7) the NRLSSI model agrees with the SATIRE and COSI models described below.

In the visible and IR range, the facular contrasts in the NRLSSI model rely on the facular model atmosphere by Solanki and Unruh (1998), which is an earlier version of the model by Unruh et al. (1999) currently used in SATIRE. Thus although the NRLSSI model does show a weak out-of-phase variability in the IR around 1600 nm (Fig. 7), integrated over the range 1000–2430 nm (Fig. 2) the modelled irradiance is in phase with the solar cycle. The SATIRE, COSI and OAR models all display reversed variability in this range. Such a reversed behaviour is also suggested by the SORCE/SIM data,

[Title Page](#)

[Abstract](#)

[Introduction](#)

[Conclusions](#)

[References](#)

[Tables](#)

[Figures](#)

[◀](#)

[▶](#)

[◀](#)

[▶](#)

[Back](#)

[Close](#)

[Full Screen / Esc](#)

[Printer-friendly Version](#)

[Interactive Discussion](#)



although the magnitude of the measured SIM variability is much stronger than in the models.

Integrated over all wavelengths, the NRLSSI irradiance (i.e. the TSI) is in good agreement with the measurements, although it does not quite reproduce the comparatively low TSI level during the last minimum in 2009 (Kopp and Lean, 2011), as indicated by the PMOD composite and also independently found by Ball et al. (2012) with the SATIRE model. This is because the Mg II index employed to describe the evolution of the bright component with time does not follow exactly the shape of the TSI variation over the last cycle (although the differences appear to be within the long-term measurement uncertainties; M. Snow, personal communication, 2012). Such a behaviour is also mimicked in some individual spectral ranges, including the 220–240 nm range (see, Fig. 8).

3.3.2 SATIRE-S

SATIRE-S³ (Spectral And Total Irradiance REconstructions for the Satellite era) belongs to the class of models using semi-empirical model atmospheres to calculate brightnesses of different surface features and full-disc solar images to describe the surface area coverage by these components at a given time. The full-disc data used in SATIRE are magnetograms and continuum images. So far, ground-based KP/NSO (Kitt Peak National Solar Observatory; 1974–2003) and space-based SOHO/MDI (Michelson Doppler Interferometer; 1996–2010) and SDO/HMI (Helioseismic and Magnetic Imager; since 2010) data have been employed. The following model atmospheres are used: the quiet Sun model by Kurucz (1991) with an effective temperature of 5777 K, similar but cooler model atmospheres for umbra and penumbra, and model P of Fontenla et al. (1999) slightly modified by Unruh et al. (1999) to achieve better agreement with observations in the visible and near-UV. Since the ATLAS9 code uses

³<http://www.mps.mpg.de/projects/sun-climate/data.html>

[Title Page](#)

[Abstract](#)

[Introduction](#)

[Conclusions](#)

[References](#)

[Tables](#)

[Figures](#)

[◀](#)

[▶](#)

[◀](#)

[▶](#)

[Back](#)

[Close](#)

[Full Screen / Esc](#)

[Printer-friendly Version](#)

[Interactive Discussion](#)



**Spectral irradiance
and climate**

I. Ermolli et al.

[Title Page](#)[Abstract](#)[Introduction](#)[Conclusions](#)[References](#)[Tables](#)[Figures](#)[◀](#)[▶](#)[◀](#)[▶](#)[Back](#)[Close](#)[Full Screen / Esc](#)[Printer-friendly Version](#)[Interactive Discussion](#)

the LTE approximation, which is known to fail in the UV, fluxes below 270 nm are rescaled using UARS/SUSIM observations (Krivova et al., 2006).

The SATIRE-S modelled variability was found to be in very good agreement, on both rotational and cyclic time scales, with the PMOD TSI composite (Wenzler et al., 2009; Ball et al., 2012), SORCE/TIM TSI measurements (Ball et al., 2011, 2012), UARS/SUSIM spectral irradiance (Krivova et al., 2006, 2009; Unruh et al., 2012), as well as with UARS/SUSIM and UARS/SOLSTICE Ly- α measurements (see also Figs. 2 and 8). On rotational times scales, good agreement is also found between the SSI provided by SATIRE-S and the SORCE/SIM and SORCE/SOLSTICE measurements (Unruh et al., 2008, 2012; Ball et al., 2011, see also bottom panel of Fig. 8) and between SATIRE-S and SOHO/VIRGO observations in three spectral channels in the near-UV, visible and near-IR (Krivova et al., 2003). Due to strong sensitivity trends, VIRGO spectral data could not be used on longer time scales. On time scales longer than a few months, the SATIRE-S trends, however, diverge significantly from those shown by SORCE/SIM and SORCE/SOLSTICE: the change in the UV is significantly weaker in SATIRE-S, and the inverse solar cycle change in the visible is not reproduced (see Figs. 7 and 8; Ball et al., 2011; Unruh et al., 2012). Interestingly, Ball et al. (2011) have shown that when integrated over the spectral range of SIM (200–1630 nm) and corrected for the missing UV and IR wavelengths, SATIRE-S still reproduces over 94 % of TSI fluctuations measured by SORCE/TIM. On time scales of months to years, the trends agree to over 99 %. At the same time, integrated SIM data show different trends, with only about 60 % of the TIM changes on these time scales being reproduced.

3.3.3 COSI

The COde for Solar Irradiance⁴ (COSI) calculates synthetic solar spectra for different components of the solar atmosphere. COSI returns the most important UV lines including the degree of ionisation of the elements under NLTE. The NLTE Opacity

⁴<ftp://ftp.pmodwrc.ch/pub/Sasha/>

Distribution Functions, implemented in COSI, indirectly account for the NLTE effects in several millions of lines. Shapiro et al. (2010) showed that NLTE effects influence the concentration of the negative ion of hydrogen which results in an approximately 10% change of the continuum level in the visible spectrum. The contrasts between active regions and the quiet Sun are also affected by the NLTE effects. This, however, does not imply that only NLTE codes are capable of reproducing the visible solar spectrum as the NLTE effects can be imitated by a slight readjustment of the atmosphere structure (see, e.g. Rutten and Kostik, 1982; Shchukina and Trujillo Bueno, 2001). The spectrum of the quiet Sun calculated with COSI is in good agreement with the solar spectrum measured by SOLSTICE (up to 320 nm) and SIM (above 320 nm) onboard the SORCE satellite during the 2008 solar minimum, and with the SOLSPEC measurements during the ATLAS 3 mission in 1994 (Thuillier et al., 2011). Shapiro et al. (2012a) showed that COSI can accurately reproduce the center-to-limb variation of solar brightness in the Herzberg continuum retrieved from the analysis of solar eclipses observed by LYRA/PROBA2.

Solar spectral irradiance variations can be modelled from COSI spectra by weighting them with filling factors of surface magnetic features (e.g. derived from the magnetograms as in the SATIRE model or from the PSPT images as in SRPM). To date, this has been done employing sunspot and ^{10}Be data (Shapiro et al., 2011) and PSPT images (Shapiro et al., 2012b, see below).

The variability so derived with COSI agrees well with SATIRE-S and NRLSSI in the Herzberg continuum spectral range (see Figs. 7 and 8) and in the visible (see Figs. 2 and 7). In the near-IR, at 700–1000 nm, COSI shows a weak inverse solar cycle variability (see Figs. 2 and 7). This is probably an artifact of the model, as Shapiro et al. (2010) calculated active-region contrasts using the model atmospheres of Fontenla et al. (1999) that do not distinguish between umbra and penumbra or between bright plage and plage. This affects the position of the inversion point; the point where the influence of sunspots starts to outweigh the bright components. To take this into account,

Spectral irradiance and climate

I. Ermolli et al.

[Title Page](#)

[Abstract](#)

[Introduction](#)

[Conclusions](#)

[References](#)

[Tables](#)

[Figures](#)

[◀](#)

[▶](#)

[◀](#)

[▶](#)

[Back](#)

[Close](#)

[Full Screen / Esc](#)

[Printer-friendly Version](#)

[Interactive Discussion](#)



Shapiro et al. (2012b) decreased plage and sunspot contrasts with respect to the quiet Sun. A more accurate approach is under development.

3.3.4 SRPM

The Solar Radiation Physical Modelling⁵ (SRPM) is a set of tools used to construct semi-empirical models of the solar atmosphere, which are used for solar irradiance reconstructions. SRPM covers all levels of the solar atmosphere from the photosphere to the corona and takes departures from the NLTE conditions into account. Seven components have been used in SRPM until recently corresponding to different features that can be identified on the Sun at a medium-resolution of ≈ 2 arcs: quiet-Sun inter-network, quiet-Sun network lane, enhanced network, plage (that is not facula), facula (i.e. very bright plage), sunspot umbra and sunspot penumbra (Fontenla et al., 2009). Recently, two additional components, namely dark quiet-Sun inter-network and hot facula, were added but not yet integrated into calculations of solar irradiance by Fontenla et al. (2011). Fontenla et al. (2011) also somewhat modified the original plage and penumbra models, to achieve better agreement with SORCE/SIM and SORCE/SOLSTICE SSI observations.

The distribution of the atmospheric components over the solar disc at a given time is derived from full-disc solar images, including images from the Precision Solar Photometric Telescopes (PSPT; Coulter and Kuhn, 1994) at the INAF Osservatorio Astronomico di Roma (Ermolli et al., 1998, 2007, 2010) and at Mauna Loa, as well as Meudon photographic images. The model presented in Fontenla et al. (2011) covers most of solar cycle 23.

Since the solar atmospheric models were specifically modified to assure better agreement with SORCE/SIM observations (including the unusually strong variability in the UV and the reversed variability in the visible), the SRPM reconstruction cannot be considered as an independent test of these data. Despite this adjustment, the UV

⁵<http://www.digidyna.com/Results2010/>

Title Page

Abstract

Introduction

Conclusions

References

Tables

Figures

◀

▶

◀

▶

Back

Close

Full Screen / Esc

Printer-friendly Version

Interactive Discussion



variability in the SRPM reconstruction is significantly weaker than what is measured by SORCE/SOLSTICE (Fontenla et al., 2011) and no detailed comparison to the SORCE data on rotational and cyclical time scales has been presented by now. Also, the observed changes of TSI on time scales longer than the solar rotation are not captured by
5 the model. The reason for this mismatch could either be that the current SPRM version is missing an additional component (as suggested in Fontenla et al. (2011), though see comments in the OAR description below), or that the temperature structure of some of the model atmospheres does not fully represent the solar atmospheric structure.

3.3.5 OAR

10 Full-disc observations carried out with the PSPT telescope in Rome (Ermolli et al., 1998, 2007, 2010) are also employed in the OAR (Osservatorio Astronomico di Roma) model of solar irradiance variations. Earlier results obtained with both a regression method and a semi-empirical model were presented by, e.g. Penza et al. (2003, 2006), Domingo et al. (2009) and Ermolli et al. (2011). A new semi-empirical model, briefly
15 outlined below, is currently under development (Ermolli et al., 2012).

Images taken between September 1997 and January 2012 have been processed and segmented to identify different features on the solar disc as described by Ermolli et al. (2010). Seven classes of atmospheric features proposed by Fontenla et al. (2009, see previous subsection) are considered, and the brightness spectrum of each feature
20 is computed using the semi-empirical atmospheric models of Fontenla et al. (2009) through the RH synthesis code (Uitenbroek, 2002).

Thus the set of components in the OAR model is essentially the same as used by
25 Fontenla et al. (2011), though their atmospheric structure is based on Fontenla et al. (2009), i.e. before the modifications to better match SORCE spectral observations. It is, therefore, particularly interesting that irradiance variations over cycle 23 computed with the OAR model are in qualitative agreement with other models and measurements, and not with the SRPM model and SORCE observations (see Fig. 2). In particular, the SSI trend in the visible (400–691 nm) over the period 2000–2012 is opposite to that

[Title Page](#)[Abstract](#)[Introduction](#)[Conclusions](#)[References](#)[Tables](#)[Figures](#)[◀](#)[▶](#)[◀](#)[▶](#)[Back](#)[Close](#)[Full Screen / Esc](#)[Printer-friendly Version](#)[Interactive Discussion](#)

measured by SORCE/SIM, and the variability in the UV (200–400 nm) is significantly weaker. Moreover, the TSI variations calculated with this model agree well with the PMOD composite and SORCE/TIM measurements on both rotational and cyclic time scales (Ermolli et al., 2012). The latter suggests that there is no need for an additional component to explain the observed TSI variability, and that the modifications to the model atmospheres made by Fontenla et al. (2011) might be the reason for the failure of the SRPM model to reproduce the TSI changes on time scales longer than the solar rotation.

3.4 Concluding remarks

10 Of the five models discussed in this section, specifically NRLSSI, SATIRE-S, COSI, SRPM and OAR, only one (SRPM) shows a behaviour qualitatively resembling that of the recent SORCE/SIM measurements, which is, however, by model design rather than an independent outcome. We note also that the integral of the SRPM SSI over the entire spectral range (i.e. the TSI) does not reproduce cyclical TSI changes (Fontenla et al., 2011).

15 The other four models are in close agreement with each other; none of them reproduces the peculiar behaviour of the UV and visible irradiance observed by SORCE/SIM (Figs. 2, 7 and 8). At the same time, these models are all in good or fair agreement with earlier UARS UV observations, TSI measurements and the model based on SCIA-MACHY data (Krivova et al., 2006, 2009; Pagaran et al., 2009; Morrill et al., 2011a; Shapiro et al., 2011; Unruh et al., 2012; Lean and DeLand, 2012; Ball et al., 2012). Interestingly, these models do agree with SORCE data on rotational times scales (e.g. Unruh et al., 2008; Ball et al., 2011; Lean and DeLand, 2012, see also bottom panel of Fig. 8). Note that good agreement on rotational time scales was also found by Deland and Cebula (2012) between SORCE and other spectral observations.

25 When comparing various models and data to each other, however, one important issue often remains unacknowledged, namely the true uncertainties in the measurements, in particular on time scales of years and longer. As an example (see also

[Title Page](#)[Abstract](#)[Introduction](#)[Conclusions](#)[References](#)[Tables](#)[Figures](#)[◀](#)[▶](#)[◀](#)[▶](#)[Back](#)[Close](#)[Full Screen / Esc](#)[Printer-friendly Version](#)[Interactive Discussion](#)

Unruh et al., 2012), we compare measured and modelled variability at 220–240 nm (Fig. 8). Over the period 2004–2008, the three models shown in this figure (NRLSSI, SATIRE-S and COSI) suggest a decrease in the integrated 220–240 nm flux of about 1 %. The fluxes measured by the SORCE/SOLSTICE and SORCE/SIM instruments in this range decreased over the same period by roughly 4 % and 7 %, respectively. In the 220–240 nm region, the accuracy and long-term stability of SORCE/SOLSTICE is considered to be better than that of SIM (Harder et al., 2010). Currently, SOLSTICE stability in this spectral range is estimated to be about 1 \% yr^{-1} (Snow et al., 2005). Thus the observed trend for SORCE/SOLSTICE (4 % over 5 yr) and its difference with the models (3 % over 5 yr), in fact, lies within the long-term instrumental uncertainty. The difference between the trends for SORCE/SIM and the models (about 6 %) is just outside the value of 5 % over 5 yr but it is known that at 220–240 SIM has lower stability than SORCE/SOLSTICE.

Despite showing much lower variability than SORCE/SIM in the UV, the models also display considerable differences between each other in the range 250–400 nm (up to a factor of three, e.g. between NRLSSI and COSI; Figs. 2 and 7). Due to the low response of UARS/SOLSTICE to variability above 220 nm and the use of rotational variability, NRLSSI underestimates the true changes in this range (Lean, 2012, personal communication), and can thus be considered as the lower limit. All other models rely on semi-empirical model atmospheres in this range, which also need further tests at all wavelengths. The differences between the models in the IR are mainly due to the lack of reliable observations of contrasts of different (solar) atmospheric components and related uncertainties in the corresponding model atmospheres. In the near-IR (700–1000 nm), all models qualitatively agree, except COSI. As discussed earlier, the inverse variability shown by COSI in this range is believed to be an artifact.

The variability of the spectral irradiance on time scales longer than the solar cycle is beyond the scope of this paper. We note, however, that uncertainties in the long-term SSI reconstructions are essentially the same as the ones discussed in this section

[Title Page](#)[Abstract](#)[Introduction](#)[Conclusions](#)[References](#)[Tables](#)[Figures](#)[|◀](#)[▶|](#)[◀](#)[▶](#)[Back](#)[Close](#)[Full Screen / Esc](#)[Printer-friendly Version](#)[Interactive Discussion](#)

convolved with the uncertainty in the magnitude of the secular change in irradiance (see, e.g. Krivova and Solanki, 2013; Schmidt et al., 2012, and references therein).

4 Climate impact of SSI measurements

This section discusses the impact of SSI variations over the solar cycle (see Fig. 1),
5 reported in recent solar observations and solar model reconstruction studies, on the atmosphere and climate. These solar induced differences in atmospheric heating rates,
ozone variability, temperature, and atmospheric circulation are investigated in recent
simulations using atmospheric models with standard solar forcing from the NRLSSI
model (e.g. SPARC-CCMVal, 2010; Taylor et al., 2012, for CMIP5 simulations). Additionally
10 a comparison to recent atmospheric model simulations using the SORCE/SIM
measurements as solar forcing (e.g. Haigh et al., 2010; Merkel et al., 2011; Oberländer
et al., 2012) is provided. As shown and discussed in the previous sections, the NRLSSI
model output and the SORCE/SIM measurements are the lower and the upper boundaries
15 of current understand of SSI solar-cycle variability. Here we aim to provide an
estimate of the magnitude of solar induced atmospheric changes in CCMs by comparing
the impact from the two opposite extremes in the current range of SSI variability.

Overview:

- The observed increase in UV irradiance at activity maximum compared to minimum results in an increase in atmospheric heating rates and correspondingly an increase in stratospheric temperatures. The larger the UV forcing the larger the direct atmospheric response.
20
- Higher UV forcing also leads to a larger surface response. The surface effect is regional and has little influence on globally averaged temperatures.
- The radiation codes in climate models need to have a spectral resolution that is high enough for the accurate representation of SSI changes in heating rates, e.g.
25



high spectral resolution in SW radiation codes. Increased resolution leads to enhanced sensitivity in the response. If the spectral resolution is not high enough, then it is essential that an accurate parameterization of the heating rates is included, otherwise the solar cycle response cannot be simulated.

- 5 – Accurate representation of ozone photochemical variations in the model simulations is important since these changes amplify the atmospheric solar signal.

4.1 Introduction

Today, the most advanced tools available for climate simulations are 3-dimensional General Circulation Models (GCMs) that numerically simulate the general circulation of 10 the atmosphere and/or the ocean based on well-established physical principles. Most climate models that are utilized for future climate predictions in the 4th IPCC report (Solomon et al., 2007) are coupled atmosphere-ocean models reaching up to the middle stratosphere (32 km), whereas CCMs that are used for future predictions of the stratospheric ozone layer in the WMO report (WMO, 2011) include interactive stratospheric chemistry and reach up to the lower mesosphere or above (80 km). The main external driving force for all climate models is the incoming solar flux at the top of the atmosphere (TOA). Currently there are two mechanisms for solar radiation influence 15 on climate, the so-called “top-down” UV effect (Kodera and Kuroda, 2002) and the “bottom-up” TSI effect (van Loon et al., 2007).

20 Even though TSI varies only by about 0.1 % over the solar cycle, larger variations of several percent occur in the UV part of the spectrum, including in the ozone absorption bands between 200 and 400 nm that are responsible at shortwave (SW) heating of the stratosphere and are important for photochemical processes (e.g. Haigh, 1994). The incoming solar irradiance at short wavelengths varies significantly with the solar 25 cycle, leading to statistically significant ozone, temperature and zonal wind solar signals in the stratosphere (Austin et al., 2008; Gray et al., 2010). These solar induced circulation changes in the stratosphere can induce noticeable decadal climate changes

[Title Page](#)[Abstract](#)[Introduction](#)[Conclusions](#)[References](#)[Tables](#)[Figures](#)[|◀](#)[▶|](#)[◀](#)[▶](#)[Back](#)[Close](#)[Full Screen / Esc](#)[Printer-friendly Version](#)[Interactive Discussion](#)

**Spectral irradiance
and climate**

I. Ermolli et al.

[Title Page](#)[Abstract](#)[Introduction](#)[Conclusions](#)[References](#)[Tables](#)[Figures](#)[|◀](#)[▶|](#)[◀](#)[▶](#)[Back](#)[Close](#)[Full Screen / Esc](#)[Printer-friendly Version](#)[Interactive Discussion](#)

Today stratospheric processes are gaining a lot of interest due to their importance for climate. Not only the effect of ozone recovery and its relationship to climate but also stratosphere-troposphere dynamical coupling and its role for predictability from days to decades have been recognized as important issues for future climate studies (e.g. Baldwin et al., 2007; Gerber et al., 2010). Therefore, a better representation of the stratosphere including improved representation of SW heating processes as well as dynamical coupling with the troposphere in global climate models is critically important.

4.2 Impact of SSI variability in climate models

The uncertainty of SSI variations in recent observations and models has significant bearing on simulations of the climate system, since the response of the atmosphere strongly depends on the spectral distribution of the solar irradiance. The effects for middle atmosphere heating, ozone chemistry and middle atmospheric temperatures are examined in the following.

4.2.1 Effects on atmospheric heating and ozone chemistry

As solar radiation is the primary source of energy that drives atmospheric as well as oceanic circulation, accurate representation of solar irradiance is of paramount importance for the simulation of the atmospheric temperature, composition and dynamics in climate models. The variability of the solar spectrum in time, and in particular over the solar cycle is necessary for the assessment of solar influence on climate. The amplitude of the simulated solar signal depends on the spectral solar fluxes prescribed at the TOA. Differences in the TOA solar irradiance spectrum result in large changes in the heating rates calculated by SW radiation schemes or radiative transfer models, as has been shown by Zhong et al. (2008) with differences of up to $\approx 1.1 \text{ K day}^{-1}$ in mid-latitude summer. Recently, Oberländer et al. (2012) examined the impact of a number of different estimates of prescribed TOA solar fluxes on the solar response in a GCM which includes a radiation scheme with enhanced spectral resolution (Nissen et al.,

I. Ermolli et al.

[Title Page](#)

[Abstract](#)

[Introduction](#)

[Conclusions](#)

[References](#)

[Tables](#)

[Figures](#)

[◀](#)

[▶](#)

[◀](#)

[▶](#)

[Back](#)

[Close](#)

[Full Screen / Esc](#)

[Printer-friendly Version](#)

[Interactive Discussion](#)



2007) and is therefore able to accurately represent the solar signal induced changes. They used the NRLSSI, the SATIRE and the SCIAMACHY solar flux input data sets, and compared their effects on SW heating rates over the 11-yr solar cycle using offline calculations. They also calculated the corresponding temperature response from 5 perpetual January GCM simulations with prescribed ozone concentrations.

The comparison revealed clear differences in SW heating rates for the solar minimum of cycle 22 (September 1986). The simulations forced with the NRLSSI reconstructions show the smallest solar heating rates. The use of the SATIRE reconstructions leads to stronger solar heating of up to 5 % in the middle and upper stratosphere. The 10 SCIAMACHY observations slightly enhance the solar heating in the mesosphere, with differences arising from the stronger solar fluxes in the Huggins bands of the SATIRE model and enhanced fluxes in the Hartley bands of the SCIAMACHY data set. Using SORCE/SIM measurements over the period May 2004 to November 2007 reveals larger changes in solar heating rates and the resulting temperatures in comparison to 15 the NRLSSI data (see also a more detailed discussion below). The lower irradiance in the visible range at higher solar activity than at minimum activity in the SORCE/SIM data does not lead to a decrease in total radiative heating.

The spectral resolution of the SW radiation scheme of EMAC-FUB has recently been extended towards a more accurate representation of the Chappuis bands (Kunze et al., 20 2012). An update of Oberländer et al. (2012), performed with the extended spectral resolution for solar minimum conditions in November 2007, separated for the UV and VIS spectral changes is presented in Fig. 9. The enhanced UV irradiance in 2004 (compared to 2007) in the SORCE/SIM data leads to higher SW heating rates while lower heating rates are simulated in the visible spectral range (Fig. 9a). The SW heating 25 rate change from 2004 to 2007 is stronger in the SORCE/SIM data than in the NRLSSI data by 0.18 K day^{-1} in the global mean (Fig. 9b). An enhanced sensitivity to changes in the Chappuis bands is found, a result which illustrates better the heating rate changes in the UV, visible and NIR spectral regions as a result from using the SORCE/SIM data.

Spectral irradiance and climate

I. Ermolli et al.

[Title Page](#)

[Abstract](#)

[Introduction](#)

[Conclusions](#)

[References](#)

[Tables](#)

[Figures](#)

[◀](#)

[▶](#)

[◀](#)

[▶](#)

[Back](#)

[Close](#)

[Full Screen / Esc](#)

[Printer-friendly Version](#)

[Interactive Discussion](#)



The range of reconstructed and measured SSI variations during the declining phase of solar cycle 23 has substantial implications for the modelling of the middle atmosphere state. The different magnitude and spectral composition of the SSI changes leads not only to a substantial alteration of heating rates considered above but also affects

- 5 photolysis rates which drive atmospheric chemistry and regulate the atmospheric ozone distribution (e.g. Brasseur and Solomon, 2005). The global ozone abundance is maintained by ozone production, destruction and transport by air motions. However, in the tropical stratosphere above ~ 30 km the ozone concentration depends primarily on photochemical processes, with oxygen photolysis playing a crucial role in atmospheric
10 chemistry. Therefore, the spectral composition and the magnitude of the SSI changes are of critical importance, since they define not only the magnitude but also the sign of the direct ozone response (e.g. Rozanov et al., 2002). The solar induced net effect of ozone in the stratosphere depends on the competition between ozone production due to oxygen photolysis in the Herzberg continuum (185–242 nm) and ozone destruction
15 caused by the ozone photolysis in the Hartley band (between 200 and 300 nm in the UV). The effects of the range of SSI estimates on stratospheric ozone as deduced by CCMs or 2-D radiative-photochemical model simulations have been recently reported in a number of papers which are described in more detail in the following paragraph.

4.2.2 Effects on ozone and temperature from atmospheric model simulations

- 20 A number of recent papers have compared the differences in response between simulations using the SORCE/SIM and NRLSSI model results. The NRLSSI is the data set widely used for climate modelling purposes, including the SPARC CCMVal (Chemistry-Climate Model Validation) and the CMIP5 simulations for the upcoming IPCC report. Haigh et al. (2010) were the first to publish the important implications of the
25 SORCE/SIM data for middle atmosphere heating and ozone with simulations from a 2-D radiative-photochemical model. A number of other studies using 3-D chemistry-climate models followed (Merkel et al., 2011; Ineson et al., 2011; Matthes, 2011; Oberländer et al., 2012; Swartz et al., 2012). To better understand the atmospheric

[Title Page](#)[Abstract](#)[Introduction](#)[Conclusions](#)[References](#)[Tables](#)[Figures](#)[|◀](#)[▶|](#)[◀](#)[▶](#)[Back](#)[Close](#)[Full Screen / Esc](#)[Printer-friendly Version](#)[Interactive Discussion](#)

sensitivity to the range of SSI estimates discussed above, these recently published model experiments using the NRLSSI and the SORCE/SIM data are compared to each other in Figs. 10 and 11 with respect to the solar signal in SW heating rates, temperatures and ozone. Additionally, so far unpublished results from the SOCOL model as well as results from three CMIP5 model experiments using the NRLSSI data set are added (see Table 2 for an overview of models and experimental designs). The purpose is to provide the reader with an initial comparison of the impacts of two SSI data sets which represent the lower and upper boundary of SSI variations. One has to keep in mind, though, that all models used slightly different experimental setups and therefore an exact comparison awaits common coordinated experiments.

Figure 10 shows the differences in SW heating rates (top) and temperatures (bottom panel) for the month of January in the tropical region, i.e. averaged between 25° S and 25° N. Differences are calculated between January of the year 2004 (during the declining phase of solar cycle 23), and January of 2007, close to solar minimum in December 2008, using the NRLSSI data (solid lines) and the SORCE/SIM and SORCE/SOLSTICE data (dashed lines).

All models listed in the upper part of Table 2, except HadGEM3, performed equilibrium simulations for the years 2004 and 2007 (Haigh et al., 2010; Oberländer et al., 2012; Merkel et al., 2011; Swartz et al., 2012). SOCOL performed a transient simulation from 2004 to 2007. Therefore the displayed differences do not provide one full solar cycle signal. The HadGEM3 model simulation used the SORCE/SIM measurements and scaled the data from 2004 to 2007 to obtain a full solar cycle signal (Ineson et al., 2011), so these differences are slightly larger than for the other models because they represent the full solar cycle signal. The simulations performed with the three CMIP5 models listed in the lower part of Table 2 represent ensemble mean time series experiments with varying solar cycle (e.g. Schmidt et al., 2012). In order to be comparable to the other equilibrium simulations, the differences shown represent the solar signal from a multiple linear regression analysis using the monthly mean TSI or Hartley band irradiance as a solar proxy. Afterwards the resulting solar signal has been

Spectral irradiance and climate

I. Ermolli et al.

[Title Page](#)

[Abstract](#)

[Introduction](#)

[Conclusions](#)

[References](#)

[Tables](#)

[Figures](#)

[◀](#)

[▶](#)

[◀](#)

[▶](#)

[Back](#)

[Close](#)

[Full Screen / Esc](#)

[Printer-friendly Version](#)

[Interactive Discussion](#)



Spectral irradiance and climate

I. Ermolli et al.

[Title Page](#)[Abstract](#)[Introduction](#)[Conclusions](#)[References](#)[Tables](#)[Figures](#)[◀](#)[▶](#)[◀](#)[▶](#)[Back](#)[Close](#)[Full Screen / Esc](#)[Printer-friendly Version](#)[Interactive Discussion](#)

other models by showing the maximum effect around 0.3 hPa, i.e. at a higher altitude than the other model simulations. In addition, the temperature response in SOCOL is always weaker using SORCE/SIM or NRLSSI data. When using SORCE/SOLSTICE data the temperature response is approximately half of the SORCE/SIM response indicating a large sensitivity of this model to different SSI data sets. Please note that the negative temperature response in SOCOL in the lower and middle stratosphere is not statistically significant. The temperature responses in the CMIP5 models closely agree with the NRLSSI equilibrium simulations.

Figure 11 displays the tropical ozone response in percent for month of January for those models that calculate ozone interactively (see Table 2). In the lower stratosphere, ozone changes induced by the forcing with SORCE/SIM data are larger and remain positive as compared to those calculated with NRLSSI data. In the middle to upper stratosphere ozone differences induced by the NRLSSI data are smaller but still positive whereas the ozone response using the SORCE/SIM data is negative. The height of the change from positive to negative ozone response varies from 5 hPa to 2 hPa between the models. Observations from 8 yr of SABER data indicate a transition altitude of about 1 hPa (Merkel et al., 2011) that is higher than for all models. This change of sign in the ozone response using SORCE data, meaning lower ozone during solar maximum than during solar minimum in the upper stratosphere, is statistically significant in all models. Swartz et al. (2012), who also examined the total ozone response and contributions from heating and photolysis, show good agreement between observations and simulations with the GEOSCCM model. Haigh et al. (2010) showed that the ozone decrease in the upper stratosphere and mesosphere is related to photochemical processes. Decreased O_3 at solar maximum is consistent with increased HO_x and O and also leads to a self-healing effect with more UV radiation reaching lower levels, enhancing O_2 photolysis and therefore increased O_3 . Additional observational evidence is needed to confirm the sign reversal in upper atmospheric ozone response.

So far the discussion focused on the response of stratospheric heating, temperatures and ozone to the forcing with NRLSSI and SORCE/SIM data. The direct solar

[Title Page](#)[Abstract](#)[Introduction](#)[Conclusions](#)[References](#)[Tables](#)[Figures](#)[◀](#)[▶](#)[◀](#)[▶](#)[Back](#)[Close](#)[Full Screen / Esc](#)[Printer-friendly Version](#)[Interactive Discussion](#)

Spectral irradiance and climate

I. Ermolli et al.

[Title Page](#)

[Abstract](#) [Introduction](#)

[Conclusions](#) [References](#)

[Tables](#) [Figures](#)

◀

▶

◀

▶

[Back](#)

[Close](#)

[Full Screen / Esc](#)

[Printer-friendly Version](#)

[Interactive Discussion](#)



Even though the solar variability on time scales longer than the 11-yr solar cycle is beyond the scope of this paper, we should note here again that the Sun is the fundamental energy source of the climate system. As such, the low solar activity in the past few years (compared to the previous 6 solar cycles), and its possible implications for future climate evolution has attracted the attention of both scientists and the public (e.g. Lockwood et al., 2010; Schrijver et al., 2011; Jones et al., 2012; Rozanov et al., 2012).

4.3 Concluding remarks

In this section we have discussed mainly the impact of NRLSSI and SORCE/SIM data, 10 the lower and upper boundaries of SSI solar cycle estimated variations, on the atmosphere and climate as depicted in chemistry-climate model simulations. The NRLSSI reconstructions provide the standard data base for simulations of the recent past and future (e.g. SPARC-CCMVal, 2010; Taylor et al., 2012). The atmospheric response with respect to this standard data set is compared to a number of different SSI estimates 15 to understand not only the single model responses but provide an estimate about the importance and robustness of solar cycle signals for climate simulations.

The importance of chemistry-climate models to adequately account for SSI changes in the radiation codes was highlighted. An enhanced spectral resolution in the radiation codes leads to enhanced sensitivity in the response. Moreover, the important role 20 of solar induced ozone changes for the amplification of solar effects on atmospheric composition, circulation and climate has been presented. Model simulations using the SORCE/SIM measurements as compared to the NRLSSI model show larger (by a factor of 2) SW heating and temperature signals. The lower irradiance in the visible range during higher solar activity than at minimum activity in the SORCE/SIM measurements 25 does not affect the increase in total radiative heating. Recent atmospheric model simulations with enhanced spectral resolution, however, point to the importance of the Chappuis bands in lower stratospheric heating. The solar ozone signal derived when the NRLSSI data are used is positive throughout the stratosphere and mesosphere,

Spectral irradiance and climate

I. Ermolli et al.

[Title Page](#)

[Abstract](#)

[Introduction](#)

[Conclusions](#)

[References](#)

[Tables](#)

[Figures](#)

[◀](#)

[▶](#)

[◀](#)

[▶](#)

[Back](#)

[Close](#)

[Full Screen / Esc](#)

[Printer-friendly Version](#)

[Interactive Discussion](#)



**Spectral irradiance
and climate**

I. Ermolli et al.

[Title Page](#)[Abstract](#)[Introduction](#)[Conclusions](#)[References](#)[Tables](#)[Figures](#)[|◀](#)[▶|](#)[◀](#)[▶](#)[Back](#)[Close](#)[Full Screen / Esc](#)[Printer-friendly Version](#)[Interactive Discussion](#)

whereas the sign is reversed in the upper stratosphere when the SORCE/SIM data are used. Observational evidence of the solar ozone signal is still limited. Observations from 8 yr of SABER and 4 yr of MLS data indicate a reversal of sign in the solar cycle ozone response in the upper atmosphere, however, the transition altitude for the sign change is higher than models suggest. This result needs to be confirmed by other satellite ozone measurements. Finally, the tropospheric and surface solar cycle response has been presented in an ensemble mean and it has been highlighted that while these changes are of minor importance for globally averaged temperatures there are larger regional responses.

We should note here that the SSI variability provided by recent observations and models is bounded by the NRLSSI model output and SORCE/SIM measurements, which are the lower and the upper boundaries, respectively. In order to better understand solar-induced climate variability and estimate uncertainties and sensitivities of single climate model responses in a more robust way, coordinated climate model simulations are needed, using a range of SSI estimates which are presented for the first time in a comprehensive way in this paper.

5 Conclusions

This paper presents an overview of our present knowledge of the impact of solar radiative forcing on the Earth's atmosphere. It covers the observations and the modelling of the solar radiative input as well as the modelling of the Earth's atmospheric response. The focus is on satellite-era (i.e. post-1970) data for which direct solar irradiance observations are routinely available. Special attention is given to the role of the UV spectral region, whose small contribution to TSI is compensated by a high relative variability with a potentially amplified influence on climate through radiative heating and ozone photochemistry.

There is today clear statistical evidence for the impact of solar variability on climate but both its magnitude and its confidence level are still subject to considerable debate.

Spectral irradiance and climate

I. Ermolli et al.

One major challenge lies in the extraction of the weak solar signal from the highly variable atmospheric state. Recent progress has been made along two directions. The first one is the assessment of the magnitude of secular trends in solar radiative forcing through the reconstruction of solar activity on centennial and millenial time scales from indirect indices such as cosmogenic isotopes, (e.g. Solanki et al., 2004; Bard and Frank, 2006; Beer et al., 2006; Usoskin, 2008; Schmidt et al., 2012). The second one, which we focus on, deals with shorter time scales, and is about recent solar variability and its impact on the lower and middle atmosphere.

The global physical mechanisms that cause the solar irradiance to change in time and eventually impact climate have been well documented, (e.g. Haigh et al., 2005; Haigh, 2007; Gray et al., 2010; Lean and Woods, 2010, and references therein). More than three decades of SSI observations are now available, but they are highly fragmented and agree poorly because of the difficulties in making radiometrically calibrated and stable measurements from space. Merging these different observations into one single and homogeneous record is a major and ongoing effort. As a consequence, several models have been developed for reproducing the SSI and its variability. The most successful ones are semi-empirical models that describe the SSI in terms of contributions coming from different solar surface magnetic features such as sunspots and faculae. Most models nowadays reproduce SSI measurements on short term time scales fairly well. However, uncertainties in SSI changes still remain on long term time scales and in the 220–400 nm band, which is of particular interest because of its impact on stratospheric ozone.

These modelled or observed variations in the SSI are today used as inputs to CCM simulations that are capable of properly reproducing most aspects of stratospheric heating and point to the existence of a significant impact of solar variability on climate. However, major uncertainties remain in their detailed description, in which nonlinear couplings and regional effects can play an important role.

The main conclusions of this joint study are:

24606

 CC BY

Interactive Discussion

© 2019 Pearson Education, Inc.

[Back](#) [Close](#)

1

Abstract	Introduction
Conclusions	References
Tables	Figures

5 – Recent SSI measurements by SORCE/SIM are hard to reconcile with earlier observations (e.g. by UARS/SOLSTICE and UARS/SUSIM) and with SSI models. SIM observations since 2004 suggest that the UV irradiance may have changed by a much larger factor than observed in the previous 3 solar cycles. Our current understanding of the causes of solar spectral variability as well as most SSI models cannot reconcile the SORCE/SIM data with other SSI and TSI observations. UV mostly affects climate through indirect heating of the stratosphere. Currently there is insufficient observational evidence to support recent SSI measurements by SORCE/SIM on the basis of comparisons between climate model simulations and atmospheric ozone or temperature observations.

10 – Within the range of recent SSI values from observations and semi-empirical models, the NRLSSI model and SORCE/SIM observations can, respectively be considered to be the lower and the upper limits in the magnitude of the solar cycle variation in the UV. The strong discrepancies in the UV are the main cause for the uncertainty in the response obtained from CCM simulations. While there has been major recent progress in better reproducing the SSI changes on short term time scales, there remains now an important issue in the derivation of realistic confidence intervals for them.

15 – The spectral and temporal coverage of the SSI gradually improved until 2004, when daily observations of the full UV, visible and near-infrared spectrum became available. Unfortunately, this situation is likely to end in 2013, with ENVISAT failing in 2012 and the future of SORCE operations limited due to an ageing battery. No complete coverage is foreseen before 2016, when the Total and Spectral Irradiance Sensor (TSIS) will be launched as part of the NOAA-NASA joint Polar Satellite System Program. This situation has led to more intensive application of semi-empirical models. There remains a considerable issue in assimilating SSI observations in such models and in reconstructing the SSI prior to the space age.

Spectral irradiance and climate

I. Ermolli et al.

[Title Page](#)

[Abstract](#)

[Introduction](#)

[Conclusions](#)

[References](#)

[Tables](#)

[Figures](#)

[◀](#)

[▶](#)

[◀](#)

[▶](#)

[Back](#)

[Close](#)

[Full Screen / Esc](#)

[Printer-friendly Version](#)

[Interactive Discussion](#)



Reconstructions going back to the early 20th century shall be available thanks to historical ground-based solar observations (e.g. Ermolli et al., 2009).

- 5 – Even though the large UV solar cycle variations as indicated by SIM/SORCE observations (Harder et al., 2009) will likely be smaller by half based upon new calibration corrections, other observations and statistical analysis of existing long-term satellite time series still show some inconsistencies in the derived SSI solar cycle variability. The main reason for this are uncertainties in the long-term stability of space observations due to degradation issues related to the hard radiation environment in space. There is certainly a need for additional and continuous SSI observations in coming years.
- 10 – TSI alone does not adequately describe the solar forcing on the atmosphere. In many climate models, the solar input still reduces to the TSI or a solar proxy that represents it, such as the f10.7 index. The TSI indeed captures most of the variability of the visible and near-infrared emissions, which represent 92 % of the incoming SW radiation and directly heat the lower atmosphere and surface. However, some SSI observations and models show that different bands of the solar spectrum do not vary in phase with the 11-yr solar sunspot cycle. Besides, for many years, the canonical value of the average TSI was $1365.4 \pm 1.3 \text{ W m}^{-2}$ whereas now the most accurate, and generally accepted, value is $1361 \pm 0.5 \text{ W m}^{-2}$ (Kopp and Lean, 2011; Schmutz et al., 2012).
- 15 – For a proper modelling of the atmospheric impact of the SSI, climate models are needed that include an adequate representation of the stratosphere and take into account the spectral nature of the incoming radiation, especially at wavelengths below 320 nm, so that the response of stratospheric heating and photolysis rates to solar irradiance variability can be represented. Early radiation codes decomposed the solar spectrum into a few spectral bands only. Recent simulations have revealed the importance of having spectrally resolving SW radiation schemes, which lead to enhanced sensitivity in the response. These models are today better

able to reproduce the salient features of the observed solar signal in the stratospheric temperatures and (in CCMs) ozone distributions.

- 5 – Results obtained with such CCMs also show that solar-driven ozone changes in the upper stratosphere amplify the direct heating of the lower atmosphere by visible and near-IR radiation. There is today a need for quantifying the impact of such feedback mechanisms, which may not only amplify the solar signature but also enhance regional effects. The top-down feedback involves various mechanisms, including the dynamical coupling between the stratosphere and the troposphere. The bottom-up feedback is mediated by the ocean-air coupling, which has recently become an active topic of investigation.

10 A unique aspect of this study is the description of the solar terrestrial connection by an interdisciplinary team of solar and atmospheric physicists. Progress on this hotly debated issue has often been hampered by the fact that limitations on observations or on models are not always properly known outside of a given scientific community. For the 15 first time a comprehensive comparison and discussion of existing SSI measurements and models is presented, as well as a first investigation of their impacts on Earth's climate. In order to reliably recommend solar forcing data sets for future climate modelling purposes, coordinated chemistry-climate model experiments using a range of the here 20 presented SSI data have to be conducted. However, it is undeniable that SSI variations and their effects on the Earth's atmosphere have to be taken into account in future climate studies.

25 *Acknowledgements.* This work has been supported by COST Action ES1005 TOSCA (<http://www.tosca-cost.eu>). We thank J. Lean and J. Fontenla for helpful comments. The authors are grateful to W. Ball, S. Criscuoli, S. Oberländer and M. Kunze for providing updated results of their work, to F. Hansen for preparing Figs. 10 to 12, and to A. Kubin, G. Chiodo, S. Misios, and A. Maycock for their active participation in the workshop of the COST Action ES1005. Our special thanks are to all instrument teams that made all the observations that were used in this study, as well as to the modelling groups that provided published and partly also unpublished data for this study, in particular to J. Haigh, S. Ineson, D. Marsh, A. Merkel, H. Schmidt, A. V.

[Title Page](#)

[Abstract](#)

[Introduction](#)

[Conclusions](#)

[References](#)

[Tables](#)

[Figures](#)

[◀](#)

[▶](#)

[◀](#)

[▶](#)

[Back](#)

[Close](#)

[Full Screen / Esc](#)

[Printer-friendly Version](#)

[Interactive Discussion](#)



**Spectral irradiance
and climate**

I. Ermolli et al.

[Title Page](#)[Abstract](#)[Introduction](#)[Conclusions](#)[References](#)[Tables](#)[Figures](#)[◀](#)[▶](#)[◀](#)[▶](#)[Back](#)[Close](#)[Full Screen / Esc](#)[Printer-friendly Version](#)[Interactive Discussion](#)

Shapiro, and W. Swartz. This work is part of the WCRP/SPARC SOLARIS initiative. E. Rozanov and A. Shapiro are supported by the Swiss National Science Foundation under grant CRSI122-130642 (FUPSOL). S. K. Solanki acknowledges support by the Korean Ministry of Education, Science and Technology (WCU grant No. R31-10016). The work of K. Matthes is supported within the Helmholtz-University Young Investigators Group NATHAN, funded by the Helmholtz Association through the President's Initiative and Networking Fund and the Helmholtz-Zentrum für Ozeanforschung Kiel (GEOMAR).

References

- Abbot, C. G., Fowle, F. E., and Aldrich, L. B.: Chapter VI., Ann. Astrophys. Observatory Smithsonian Inst., 4, 177–215, 1923. 24574
- Afram, N., Unruh, Y. C., Solanki, S. K., Schüssler, M., Lagg, A., and Vögler, A.: Intensity contrast from MHD simulations and HINODE observations, Astron. Astrophys., 526, A120, doi:10.1051/0004-6361/201015582, 2011. 24584
- Amblard, P.-O., Moussaoui, S., Dudok de Wit, T., Aboudarham, J., Kretzschmar, M., Lilenstein, J., and Auchère, F.: The EUV Sun as the superposition of elementary Suns, Astron. Astrophys., 487, L13–L16, doi:10.1051/0004-6361:200809588, 2008. 24573
- Austin, J., Tourpali, K., Rozanov, E., Akiyoshi, H., Bekki, S., Bodeker, G., Brühl, C., Butchart, N., Chipperfield, M., Deushi, M., Fomichev, V. I., Giorgetta, M. A., Gray, L., Kodera, K., Lott, F., Manzini, E., Marsh, D., Matthes, K., Nagashima, T., Shibata, K., Stolarski, R. S., Struthers, H., and Tian, W.: Coupled chemistry climate model simulations of the solar cycle in ozone and temperature, J. Geophys. Res.-Atmos., 113, D11306, doi:10.1029/2007JD009391, 2008. 24595
- Avrett, E. H. and Loeser, R.: Models of the solar chromosphere and transition region from SUMER and HRTS observations: formation of the extreme-ultraviolet spectrum of hydrogen, carbon, and oxygen, Astrophys. J. Suppl. S., 175, 229–276, doi:10.1086/523671, 2008. 24584
- Baldwin, M., Dameris, M., Austin, J., Bekki, S., Bregman, B., Butchart, N., Cordero, E., Gillett, N., Graf, H., Granier, C., Kinnison, D., Lal, S., Peter, T., Randel, W., Scinocca, J., Shindell, D., Struthers, H., Takahashi, M., and Thompson, D.: Climate-ozone connections, in: Scientific Assesment of Ozone Depletion: 2006, Global Ozone Research and Monitoring

- 5 Ball, W. T., Unruh, Y. C., Krivova, N. A., Solanki, S., and Harder, J. W.: Solar irradiance variability: a six-year comparison between SORCE observations and the SATIRE model, *Astron. Astrophys.*, 530, A71, doi:10.1051/0004-6361/201016189, 2011. 24561, 24583, 24588, 24592
- Ball, W. T., Unruh, Y. C., Krivova, N. A., Solanki, S., Wenzler, T., Mortlock, D. J., and Jaffe, A. H.: Reconstruction of total solar irradiance 1974–2009, *Astron. Astrophys.*, 541, A27, doi:10.1051/0004-6361/201118702, 2012. 24579, 24582, 24583, 24587, 24588, 24592
- 10 Balmaceda, L. A., Solanki, S. K., Krivova, N. A., and Foster, S.: A homogeneous database of sunspot areas covering more than 130 years, *J. Geophys. Res.-Space*, 114, A07104, doi:10.1029/2009JA014299, 2009. 24567
- Bard, E. and Frank, M.: Climate change and solar variability: what's new under the Sun?, *Earth Planet. Sci. Lett.*, 248, 1–14, doi:10.1016/j.epsl.2006.06.016, 2006. 24606
- 15 Beer, J., Vonmoos, M., and Muscheler, R.: Solar variability over the past several millennia, *Space Sci. Rev.*, 125, 67–79, doi:10.1007/s11214-006-9047-4, 2006. 24606
- Bovensmann, H., Burrows, J. P., Buchwitz, M., Frerick, J., Noël, S., Rozanov, V. V., Chance, K. V., and Goede, A. P. H.: SCIAMACHY: mission objectives and measurement modes, *J. Atmos. Sci.*, 56, 127–150, doi:10.1175/1520-0469(1999)056<0127:SMOAMM>2.0.CO;2, 1999. 24565, 24567
- 20 Bovensmann, H., Aben, I., van Roozendael, M., Kühl, S., Gottwald, M., von Savigny, C., Buchwitz, M., Richter, A., Frankenberg, C., Stammes, P., de Graaf, M., Wittrock, F., Sinnhuber, B. M., Schönhardt, A., Beirle, S., Gloudemans, A., Schrijver, H., Bracher, A., Rozanov, A. V., Weber, M., and Burrows, J. P.: SCIAMACHY's view of the changing earth's environment, Chap. 10, in: SCIAMACHY – Exploring the Changing Earth's Atmosphere, edited by: Gottwald, M. and Bovensmann, H., Springer, Dordrecht, 2011. 24567
- 25 Brasseur, G. P. and Solomon, S.: Aeronomy of the middle atmosphere: chemistry and physics of the stratosphere and mesosphere, in: Aeronomy of the Middle Atmosphere: Chemistry and Physics of the Stratosphere and Mesosphere, 2005 XII, pp. 644, 3rd rev. and enlarged edn. 1-4020-3284-6, edited by: Brasseur, G. P. and Solomon, S., Springer, Berlin, 2005. 24599
- 30 Brueckner, G. E., Edlow, K. L., Floyd, IV, L. E., Lean, J. L., and Vanhoosier, M. E.: The solar ultraviolet spectral irradiance monitor (SUSIM) experiment on board the Upper Atmosphere Research Satellite (UARS), *J. Geophys. Res.*, 98, 10695–10711, doi:10.1029/93JD00410, 1993. 24566

[Title Page](#)

[Abstract](#)

[Introduction](#)

[Conclusions](#)

[References](#)

[Tables](#)

[Figures](#)

[◀](#)

[▶](#)

[◀](#)

[▶](#)

[Back](#)

[Close](#)

[Full Screen / Esc](#)

[Printer-friendly Version](#)

[Interactive Discussion](#)



- Burrows, J. P., Weber, M., Buchwitz, M., Rozanov, V., Ladstätter-Weißenmayer, A., Richter, A., Debeek, R., Hoogen, R., Bramstedt, K., Eichmann, K.-U., Eisinger, M., and Perner, D.: The Global Ozone Monitoring Experiment (GOME): mission concept and first scientific results, *J. Atmos. Sci.*, 56, 151–175, doi:10.1175/1520-0469(1999)056<0151:TGOME>2.0.CO;2, 1999. 24565, 24567
- Butler, J. J., Johnson, B. C., Price, K. P., Shirley, E. L., and Barnes, R. A.: Sources of differences in on-orbital total solar irradiance measurements and description of a proposed laboratory intercomparison, *J. Res. Natl. Inst. Stan.*, 113, 187–203, doi:10.6028/jres.113.014, 2008. 24576
- Cahalan, R. F., Wen, G., Harder, J. W., and Pilewskie, P.: Temperature responses to spectral solar variability on decadal time scales, *Geophys. Res. Lett.*, 37, L07705, doi:10.1029/2009GL041898, 2010. 24562
- Calisesi, Y., Bonnet, R.-M., Gray, L., Langen, J., and Lockwood, M.: Solar variability and planetary climates, vol. 23 of Space Sciences Series of ISSI, Springer Verlag, Berlin, doi:10.1007/978-0-387-48341-2, 2007. 24560
- Carlsson, M. and Stein, R. F.: Formation of solar calcium H and K bright grains, *Astrophys. J.*, 481, 500–514, doi:10.1086/304043, 1997. 24584
- Cebula, R. P., DeLand, M. T., and Hilsenrath, E.: NOAA 11 solar backscattered ultraviolet, model 2 (SBUV/2) instrument solar spectral irradiance measurements in 1989–1994 1. Observations and long-term calibration, *J. Geophys. Res.*, 103, 16235–16250, doi:10.1029/98JD01205, 1998. 24565
- Chapman, G. A., Cookson, A. M., and Dobias, J. J.: Variations in total solar irradiance during solar cycle 22, *J. Geophys. Res.*, 101, 13541–13548, doi:10.1029/96JA00683, 1996. 24579, 24583
- Chapman, G. A., Cookson, A. M., and Preminger, D. G.: Comparison of TSI from SORCE TIM with SFO ground-based photometry, *Sol. Phys.*, 276, 35–41, doi:10.1007/s11207-011-9867-6, 2012. 24583
- Coulter, R. L. and Kuhn, J. R.: RISE/PSPT as an experiment to study active region irradiance and luminosity evolution, in: Solar active region evolution: comparing models with observations. Astronomical Society of the Pacific Conference Series, volume 68, Proceedings of the Fourteenth (14th) International Summer Workshop, National Solar Observatory/Sacramento Peak, Sunspot, New Mexico, USA, 30 August–3 September 1993, San Francisco: Astronom-

Spectral irradiance and climate

I. Ermolli et al.

[Title Page](#)[Abstract](#)[Introduction](#)[Conclusions](#)[References](#)[Tables](#)[Figures](#)[◀](#)[▶](#)[◀](#)[▶](#)[Back](#)[Close](#)[Full Screen / Esc](#)[Printer-friendly Version](#)[Interactive Discussion](#)

- ical Society of the Pacific (ASP), edited by: Balasubramaniam, K. S. and Simon, G. W., p. 37, 1994. 24590
- Deland, M. T. and Cebula, R. P.: Composite MG II solar activity index for solar cycles 21 and 22, *J. Geophys. Res.*, 98, 12809–12823, doi:10.1029/93JD00421, 1993. 24566
- 5 DeLand, M. T. and Cebula, R. P.: Creation of a composite solar ultraviolet irradiance data set, *J. Geophys. Res.-Space*, 113, A11103, doi:10.1029/2008JA013401, 2008. 24566, 24572, 24579
- Deland, M. T. and Cebula, R. P.: Solar UV variations during the decline of cycle 23, *J. Atmos. Sol.-Terr. Phys.*, 77, 225–234, doi:10.1016/j.jastp.2012.01.007, 2012. 24561, 24570, 24592
- 10 Deland, M. T., Floyd, L. E., Rottman, G. J., and Pap, J. M.: Status of UARS solar UV irradiance data, *Adv. Space Res.*, 34, 243–250, doi:10.1016/j.asr.2003.03.043, 2004. 24565
- Domingo, V., Ermolli, I., Fox, P., Fröhlich, C., Haberreiter, M., Krivova, N., Kopp, G., Schmutz, W., Solanki, S. K., Spruit, H. C., Unruh, Y., and Vögler, A.: Solar surface magnetism and irradiance on time scales from days to the 11-year cycle, *Space Sci. Rev.*, 145, 15 337–380, doi:10.1007/s11214-009-9562-1, 2009. 24591
- Donnelly, R. F., Heath, D. F., and Lean, J. L.: Active-region evolution and solar rotation variations in solar UV irradiance, total solar irradiance, and soft X-rays, *J. Geophys. Res.*, 87, 10318–10324, 1982. 24583
- 20 Dudok de Wit, T.: A method for filling gaps in solar irradiance and solar proxy data, *Astron. Astrophys.*, 533, A29, doi:10.1051/0004-6361/201117024, 2011. 24573
- Dudok de Wit, T., Kretzschmar, M., Liliensten, J., and Woods, T.: Finding the best proxies for the solar UV irradiance, *Geophys. Res. Lett.*, 36, L10107, doi:10.1029/2009GL037825, 2009. 24566
- Eddy, J. A., Gilliland, R. L., and Hoyt, D. V.: Changes in the solar constant and climatic effects, 25 *Nature*, 300, 689–693, doi:10.1038/300689a0, 1982. 24582
- Egorova, T., Rozanov, E., Manzini, E., Haberreiter, M., Schmutz, W., Zubov, V., and Peter, T.: Chemical and dynamical response to the 11-year variability of the solar irradiance simulated with a chemistry-climate model, *Geophys. Res. Lett.*, 31, L06119, doi:10.1029/2003GL019294, 2004. 24596
- 30 Ermolli, I., Fofi, M., Bernacchia, C., Berrilli, F., Caccin, B., Egidi, A., and Florio, A.: The prototype RISE-PSPT instrument operating in Rome, *Sol. Phys.*, 177, 1–10, 1998. 24590, 24591

[Title Page](#)[Abstract](#)[Introduction](#)[Conclusions](#)[References](#)[Tables](#)[Figures](#)[◀](#)[▶](#)[◀](#)[▶](#)[Back](#)[Close](#)[Full Screen / Esc](#)[Printer-friendly Version](#)[Interactive Discussion](#)

**Spectral irradiance
and climate**

I. Ermolli et al.

[Title Page](#)[Abstract](#)[Introduction](#)[Conclusions](#)[References](#)[Tables](#)[Figures](#)[◀](#)[▶](#)[◀](#)[▶](#)[Back](#)[Close](#)[Full Screen / Esc](#)[Printer-friendly Version](#)[Interactive Discussion](#)

**Spectral irradiance
and climate**

I. Ermolli et al.

[Title Page](#)[Abstract](#)[Introduction](#)[Conclusions](#)[References](#)[Tables](#)[Figures](#)[◀](#)[▶](#)[◀](#)[▶](#)[Back](#)[Close](#)[Full Screen / Esc](#)[Printer-friendly Version](#)[Interactive Discussion](#)

in Geospace, vol. 415 of ESA Special Publication, edited by: Wilson, A., European Space Agency, Noordwijk, The Netherlands, 227, 1997. 24579, 24583

Fröhlich, C. and Lean, J.: The Sun's total irradiance: cycles, trends and related climate change uncertainties since 1976, *Geophys. Res. Lett.*, 25, 4377–4380, doi:10.1029/1998GL900157, 1998. 24575

Fröhlich, C. and Lean, J.: Solar radiative output and its variability: evidence and mechanisms, *Astron. Astrophys. Rev.*, 12, 273–320, doi:10.1007/s00159-004-0024-1, 2004. 24560, 24586

Fröhlich, C., Andersen, B. N., Appourchaux, T., Berthomieu, G., Crommelynck, D. A., Domingo, V., Fichot, A., Finsterle, W., Gomez, M. F., Gough, D., Jimenez, A., Leifsen, T., Lombaerts, M., Pap, J. M., Provost, J., Cortes, T. R., Romero, J., Roth, H., Sekii, T., Telljohann, U., Toutain, T., and Wehrli, C.: First results from VIRGO, the experiment for helioseismology and solar irradiance monitoring on SOHO, *Sol. Phys.*, 170, 1–25, 1997. 24565, 24629

Garcia, R. R.: Atmospheric physics: solar surprise?, *Nature*, 467, 668–669, doi:10.1038/467668a, 2010. 24562

Gerber, E. P., Baldwin, M. P., Akiyoshi, H., Austin, J., Bekki, S., Braesicke, P., Butchart, N., Chipperfield, M., Dameris, M., Dhomse, S., Frith, S. M., Garcia, R. R., Garny, H., Gettelman, A., Hardiman, S. C., Karpechko, A., Marchand, M., Morgenstern, O., Nielsen, J. E., Pawson, S., Peter, T., Plummer, D. A., Pyle, J. A., Rozanov, E., Scinocca, J. F., Shepherd, T. G., and Smale, D.: Stratosphere-troposphere coupling and annular mode variability in chemistry-climate models, *J. Geophys. Res.-Atmos.*, 115, D00M06, doi:10.1029/2009JD013770, 2010. 24597

Gray, L. J., Beer, J., Geller, M., Haigh, J. D., Lockwood, M., Matthes, K., Cubasch, U., Fleitmann, D., Harrison, G., Hood, L., Luterbacher, J., Meehl, G. A., Shindell, D., van Geel, B., and White, W.: Solar influences on climate, *Rev. Geophys.*, 48, RG4001, doi:10.1029/2009RG000282, 2010. 24560, 24595, 24606

Grossmann-Doerth, U., Knoelker, M., Schuessler, M., and Solanki, S. K.: The deep layers of solar magnetic elements, *Astron. Astrophys.*, 285, 648–654, 1994. 24580

Haigh, J. D.: The role of stratospheric ozone in modulating the solar radiative forcing of climate, *Nature*, 370, 544–546, doi:10.1038/370544a0, 1994. 24595

Haigh, J. D.: A GCM study of climate change in response to the 11-year solar cycle, *Q. J. Roy. Meteor. Soc.*, 125, 871–892, doi:10.1002/qj.49712555506, 1999. 24596, 24603

Spectral irradiance
and climate

I. Ermolli et al.

[Title Page](#)

[Abstract](#)

[Introduction](#)

[Conclusions](#)

[References](#)

[Tables](#)

[Figures](#)

◀

▶

◀

▶

[Back](#)

[Close](#)

[Full Screen / Esc](#)

[Printer-friendly Version](#)

[Interactive Discussion](#)



Spectral irradiance and climate

I. Ermolli et al.

[Title Page](#)[Abstract](#)[Introduction](#)[Conclusions](#)[References](#)[Tables](#)[Figures](#)[◀](#)[▶](#)[◀](#)[▶](#)[Back](#)[Close](#)[Full Screen / Esc](#)[Printer-friendly Version](#)[Interactive Discussion](#)

- 5 Jain, K. and Hasan, S. S.: Modulation in the solar irradiance due to surface magnetism during cycles 21, 22 and 23, *Astron. Astrophys.*, 425, 301–307, doi:10.1051/0004-6361:20047102, 2004. 24583
- 10 Jones, G. S., Lockwood, M., and Stott, P. A.: What influence will future solar activity changes over the 21st century have on projected global near-surface temperature changes?, *J. Geophys. Res.-Atmos.*, 117, D05103, doi:10.1029/2011JD017013, 2012. 24604
- Keller, C. U., Schüssler, M., Vögler, A., and Zakharov, V.: On the origin of solar faculae, *Astrophys. J.*, 607, L59–L62, doi:10.1086/421553, 2004. 24580
- 15 Kobel, P., Solanki, S. K., and Borrero, J. M.: The continuum intensity as a function of magnetic field. I. Active region and quiet Sun magnetic elements, *Astron. Astrophys.*, 531, A112, doi:10.1051/0004-6361/201016255, 2011. 24582
- Kodera, K.: Solar cycle modulation of the North Atlantic Oscillation: implication in the spatial structure of the NAO, *Geophys. Res. Lett.*, 29, 1218, doi:10.1029/2001GL014557, 2002. 24596, 24603
- 20 Kodera, K. and Kuroda, Y.: Dynamical response to the solar cycle, *J. Geophys. Res.-Atmos.*, 107, 4749, doi:10.1029/2002JD002224, 2002. 24562, 24595
- Kopp, G. and Lean, J. L.: A new, lower value of total solar irradiance: evidence and climate significance, *Geophys. Res. Lett.*, 38, L01706, doi:10.1029/2010GL045777, 2011. 24571, 24574, 24575, 24576, 24587, 24608
- 25 Kopp, G., Lawrence, G., and Rottman, G.: The Total Irradiance Monitor (TIM): Science Results, *Sol. Phys.*, 230, 129–139, doi:10.1007/s11207-005-7433-9, 2005. 24568
- Krivova, N. A. and Solanki, S. K.: Models of solar total and spectral irradiance variability of relevance for climate studies, in: Climate and Weather of the Sun–Earth System (CAWSES): highlights from a priority program, edited by: Lübken, F.-J., Springer, Dordrecht, The Netherlands, 19–38, 10.1007/978-94-007-4348-9_2, 2013. 24594, 24632
- 30 Krivova, N. A., Solanki, S. K., Fligge, M., and Unruh, Y. C.: Reconstruction of solar irradiance variations in cycle 23: Is solar surface magnetism the cause?, *Astron. Astrophys.*, 399, L1–L4, doi:10.1051/0004-6361:20030029, 2003. 24579, 24583, 24588
- Krivova, N. A., Solanki, S. K., and Floyd, L.: Reconstruction of solar UV irradiance in cycle 23, *Astron. Astrophys.*, 452, 631–639, doi:10.1051/0004-6361:20064809, 2006. 24561, 24570, 24585, 24588, 24592, 24638

Spectral irradiance and climate

I. Ermolli et al.

[Title Page](#)

[Abstract](#)

[Introduction](#)

[Conclusions](#)

[References](#)

[Tables](#)

[Figures](#)

[◀](#)

[▶](#)

[◀](#)

[▶](#)

[Back](#)

[Close](#)

[Full Screen / Esc](#)

[Printer-friendly Version](#)

[Interactive Discussion](#)



- Krivova, N. A., Balmaceda, L., and Solanki, S. K.: Reconstruction of solar total irradiance since 1700 from the surface magnetic flux, *Astron. Astrophys.*, 467, 335–346, doi:10.1051/0004-6361:20066725, 2007. 24583
- Krivova, N. A., Solanki, S. K., Wenzler, T., and Podlipnik, B.: Reconstruction of solar UV irradiance since 1974, *J. Geophys. Res.-Atmos.*, 114, D00I04, doi:10.1029/2009JD012375, 2009. 5 24585, 24588, 24592, 24638
- Krivova, N. A., Vieira, L. E. A., and Solanki, S. K.: Reconstruction of solar spectral irradiance since the Maunder minimum, *J. Geophys. Res.-Space*, 115, A12112, doi:10.1029/2010JA015431, 2010. 24583
- Kunze, M., Godolt, M., Heimann-Reinus, A., Langematz, U., Grenfell, J. L., and Rauer, H.: Investigating the early Earth faint young Sun problem with a general circulation model, *Planet. Space Sci.*, submitted, 2012. 10 24598
- Kuroda, Y.: Relationship between the Polar-night jet oscillation and the annular mode, *Geophys. Res. Lett.*, 29, 1240, doi:10.1029/2001GL013933, 2002. 24603
- Kurucz, R. L.: New opacity calculations, in: *NATO ASIC Proc. 341: Stellar Atmospheres – Beyond Classical Models*, edited by: Crivellari, L., Hubeny, I., and Hummer, D. G., Dordrecht, D. Reidel Publishing Co., p. 441, 1991. 15 24586, 24587
- Kurucz, R. L.: ATLAS9 Stellar Atmosphere Programs and 2 km s^{-1} grid., ATLAS9 Stellar Atmosphere Programs and 2 km s^{-1} grid, Kurucz CD-ROM No. 13, Smithsonian Astrophysical Observatory, Cambridge, Mass., 1993. 20 24584
- Kurucz, R. L.: ATLAS12, SYNTHE, ATLAS9, WIDTH9, et cetera, *Mem. Soc. Astron. Ital. Suppl.*, 8, 14, 2005. 24584
- Langematz, U., Kubin, A., Brühl, C., Baumgaertner, A., Cubasch, U., and Spangehl, T.: Solar effects on chemistry and climate including ocean interactions, in: *Climate and Weather of the Earth System (CAWSES)*, edited by: Lübken, F., 541–572, Springer, Dordrecht, The Netherlands, 2013. 25 24603
- Lawrence, G. M., Rottman, G., Harder, J., and Woods, T.: Solar total irradiance monitor (TIM), *Metrologia*, 37, 407, doi:10.1088/0026-1394/37/5/13, 2000. 30 24629
- Lawrence, G. M., Kopp, G., Rottman, G., Harder, J., Woods, T., and Loui, H.: Calibration of the total irradiance monitor, *Metrologia*, 40, S78–S80, doi:10.1088/0026-1394/40/1/317, 2003. 24575
- Lean, J. L.: The Sun's variable radiation and its relevance for Earth, *Annu. Rev. Astron. Astr.*, 35, 33–67, doi:10.1146/annurev.astro.35.1.33, 1997. 24566

Spectral irradiance and climate

I. Ermolli et al.

[Title Page](#)[Abstract](#)[Introduction](#)[Conclusions](#)[References](#)[Tables](#)[Figures](#)[◀](#)[▶](#)[◀](#)[▶](#)[Back](#)[Close](#)[Full Screen / Esc](#)[Printer-friendly Version](#)[Interactive Discussion](#)

- Lean, J. L.: Evolution of the Sun's spectral irradiance since the Maunder minimum, *Geophys. Res. Lett.*, 27, 2425–2428, doi:10.1029/2000GL000043, 2000. 24561, 24583, 24585, 24586
- Lean, J. L. and DeLand, M. T.: How does the Sun's spectrum vary?, *J. Climate*, 25, 2555–2560, doi:10.1175/JCLI-D-11-00571.1, 2012. 24561, 24574, 24592
- Lean, J. L. and Woods, T. N.: Solar total and spectral irradiance measurements and models, in: *Evolving Solar Physics and the Climates of Earth and Space*, edited by: Schrijver, C. J. and Siscoe, G. L., Cambridge University Press, Cambridge, 2010. 24606
- Lean, J. L., Livingston, W. C., Heath, D. F., Donnelly, R. F., Skumanich, A., and White, O. R.: A three-component model of the variability of the solar ultraviolet flux 145–200 nm, *J. Geophys. Res.*, 87, 10307–10317, doi:10.1029/JA087iA12p10307, 1982. 24573
- Lean, J. L., Rottman, G. J., Kyle, H. L., Woods, T. N., Hickey, J. R., and Puga, L. C.: Detection and parameterization of variations in solar mid- and near-ultraviolet radiation (200–400 nm), *J. Geophys. Res.*, 102, 29939–29956, doi:10.1029/97JD02092, 1997. 24561, 24585, 24586
- Lee, III, R. B., Barkstrom, B. R., and Cess, R. D.: Characteristics of the Earth radiation budget experiment solar monitors, *Appl. Optics*, 26, 3090–3096, doi:10.1364/AO.26.003090, 1987. 24629
- Lee, III, R. B., Gibson, M. A., Wilson, R. S., and Thomas, S.: Long-term total solar irradiance variability during sunspot cycle 22, *J. Geophys. Res.*, 100, 1667–1675, doi:10.1029/94JA02897, 1995. 24575
- Lockwood, M.: Was UV spectral solar irradiance lower during the recent low sunspot minimum?, *J. Geophys. Res.-Atmos.*, 116, D16103, doi:10.1029/2010JD014746, 2011. 24572
- Lockwood, M.: Solar influence on global and regional climates, *Surv. Geophys.*, 33, 503–534, doi:10.1007/s10712-012-9181-3, 2012. 24560
- Lockwood, M., Harrison, R. G., Woollings, T., and Solanki, S. K.: Are cold winters in Europe associated with low solar activity?, *Environ. Res. Lett.*, 5, 024001, doi:10.1088/1748-9326/5/2/024001, 2010. 24604
- Loukitcheva, M., Solanki, S. K., Carlsson, M., and Stein, R. F.: Millimeter observations and chromospheric dynamics, *Astron. Astrophys.*, 419, 747–756, doi:10.1051/0004-6361:20034159, 2004. 24584
- Matthes, K.: Atmospheric science: solar cycle and climate predictions, *Nat. Geosci.*, 4, 735–736, doi:10.1038/ngeo1298, 2011. 24596, 24599

Spectral irradiance and climate

I. Ermolli et al.

[Title Page](#)[Abstract](#)[Introduction](#)[Conclusions](#)[References](#)[Tables](#)[Figures](#)[◀](#)[▶](#)[◀](#)[▶](#)[Back](#)[Close](#)[Full Screen / Esc](#)[Printer-friendly Version](#)[Interactive Discussion](#)

**Spectral irradiance
and climate**

I. Ermolli et al.

[Title Page](#)[Abstract](#)[Introduction](#)[Conclusions](#)[References](#)[Tables](#)[Figures](#)[◀](#)[▶](#)[◀](#)[▶](#)[Back](#)[Close](#)[Full Screen / Esc](#)[Printer-friendly Version](#)[Interactive Discussion](#)

Pagaran, J., Weber, M., Deland, M. T., Floyd, L. E., and Burrows, J. P.: Solar spectral irradiance variations in 240–1600 nm during the recent solar cycles 21–23, *Sol. Phys.*, 272, 159–188, doi:10.1007/s11207-011-9808-4, 2011b. 24567, 24568

5 Pap, J. M., Willson, R. C., Froelich, C., Donnelly, R. F., and Puga, L.: Long-term variations in total solar irradiance, *Sol. Phys.*, 152, 13–21, doi:10.1007/BF01473177, 1994. 24629

Pap, J. M., Fox, P., Fröhlich, C., Hudson, H. S., Kuhn, J., McCormack, J., North, G., Sprigg, W., and Wu, S. T. (Eds.): *Solar Variability and its Effects on Climate*, vol. 141 of Geophysical Monograph Series, American Geophysical Union, Washington DC, 2004. 24560

10 Penza, V., Caccin, B., Ermolli, I., Centrone, M., and Gomez, M. T.: Modeling solar irradiance variations through PSPT images and semiempirical models, in: *Solar Variability as an Input to the Earth's Environment*, vol. 535 of ESA Special Publication, edited by: Wilson, A., European Space Agency, ESA Publications Division, Noordwijk, The Netherlands, ISBN 92-9092-845-X, 299–302, 2003. 24591

15 Penza, V., Caccin, B., Ermolli, I., and Centrone, M.: Comparison of model calculations and photometric observations of bright “magnetic” regions, *Astron. Astrophys.*, 413, 1115–1123, doi:10.1051/0004-6361:20031397, 2004. 24584

Penza, V., Pietropaolo, E., and Livingston, W.: Modeling the cyclic modulation of photospheric lines, *Astron. Astrophys.*, 454, 349–358, doi:10.1051/0004-6361:20053405, 2006. 24591

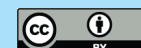
20 Preminger, D. G., Walton, S. R., and Chapman, G. A.: Photometric quantities for solar irradiance modeling, *J. Geophys. Res.-Space*, 107, 1354, doi:10.1029/2001JA009169, 2002. 24579, 24583

Röhrbein, D., Cameron, R., and Schüssler, M.: Is there a non-monotonic relation between photospheric brightness and magnetic field strength in solar plage regions?, *Astron. Astrophys.*, 532, A140, doi:10.1051/0004-6361/201117090, 2011. 24582

25 Rottman, G.: The SORCE mission, *Sol. Phys.*, 230, 7–25, doi:10.1007/s11207-005-8112-6, 2005. 24561, 24568

Rottman, G., Woods, T., Snow, M., and Detoma, G.: The solar cycle variation in ultraviolet irradiance, *Adv. Space Res.*, 27, 1927–1932, doi:10.1016/S0273-1177(01)00272-1, 2001. 24565

30 Rottman, G., Floyd, L., and Viereck, R.: Measurement of the solar ultraviolet irradiance, in: *Solar Variability and its Effects on Climate*, Geophysical Monograph 141, edited by: Pap, J. M., Fox, P., Fröhlich, C., Hudson, H. S., Kuhn, J., McCormack, J., North, G., Sprigg, W., and Wu, S. T., American Geophysical Union, Washington DC, 111–125, 2004. 24565

[Title Page](#)[Abstract](#)[Introduction](#)[Conclusions](#)[References](#)[Tables](#)[Figures](#)[◀](#)[▶](#)[◀](#)[▶](#)[Back](#)[Close](#)[Full Screen / Esc](#)[Printer-friendly Version](#)[Interactive Discussion](#)

Rottman, G. J., Woods, T. N., and Sparn, T. P.: Solar–stellar irradiance comparison experiment 1. I – instrument design and operation, *J. Geophys. Res.*, 98, 10667, doi:10.1029/93JD00462, 1993. 24569

Rozanov, E., Egorova, T., Fröhlich, C., Haberreiter, M., Peter, T., and Schmutz, W.: Estimation of the ozone and temperature sensitivity to the variation of spectral solar flux, in: From Solar Min to Max: Half a Solar Cycle with SOHO, vol. 508 of ESA Special Publication, edited by: Wilson, A., European Space Agency, ESA Publications Division, Noordwijk, The Netherlands. ISBN 92-9092-818-2, 181–184. 2002. 24573. 24599

Rozanov, E. V., Egorova, T. A., Shapiro, A. I., and Schmutz, W. K.: Modeling of the atmospheric response to a strong decrease of the solar activity, IAU Symp., 286, 215–224, doi:10.1017/S1743921312004863. 2012, 24604

Rutten, R. J.: Radiative Transfer in Stellar Atmospheres, University of Utrecht, Utrecht, The Netherlands, 2003. 24584

Rutten, R. J. and Kostik, R. I.: Empirical NLTE analyses of solar spectral lines, III – iron lines versus LTE models of the photosphere, *Astron. Astrophys.*, 115, 104–114, 1982. 24589

Schmidt, G. A., Jungclaus, J. H., Ammann, C. M., Bard, É., Braconnot, P., Crowley, T. J., Delaigue, G., Joos, F., Krivova, N. A., Muscheler, R., Otto-Bliesner, B. L., Pongratz, J., Shindell, D. T., Solanki, S. K., Steinhilber, F., and Vieira, L. E. A.: Climate forcing reconstructions for use in PMIP simulations of the Last Millennium (v1.1), *Geosci. Model Dev.*, 5, 185–191, doi:10.5194/gmd-5-185-2012, 2012. 24594, 24600, 24606

Schmutz, W., Fehlmann, A., Hülsen, G., Meindl, P., Winkler, R., Thuillier, G., Blattner, P., Buisson, F., Egorova, T., Finsterle, W., Fox, N., Gröbner, J., Hochedez, J.-F., Koller, S., Meftafah, M., Meisonnier, M., Nyeki, S., Pfiffner, D., Roth, H., Rozanov, E., Spescha, M., Wehrli, C., Werner, L., and Wyss, J. U.: The PREMOS/PICARD instrument calibration, *Metrologia*, 46, 202 doi:10.1088/0026-1394/46/4/S13 2009 24575 24629

Schmutz, W., Fehlmann, A., Finsterle, W., and the PREMOS team: First Light of PREMOS/PICARD, Annual Report 2011, Physikalisch-Meteorologisches Observatorium, World Radiation Center, Davos, Switzerland, http://www.pmodwrc.ch/annual_report/annualreport2011.pdf, 44 pp., 2012. 24574, 24575, 24576, 24608

30 Schraner, M., Rozanov, E., Schnadt Poberaj, C., Kenzelmann, P., Fischer, A. M., Zubov, V., Luo, B. P., Hoyle, C. R., Egorova, T., Fueglistaler, S., Brönnimann, S., Schmutz, W., and Peter, T.: Technical Note: Chemistry-climate model SOCOL: version 2.0 with improved transport and

chemistry/microphysics schemes, *Atmos. Chem. Phys.*, 8, 5957–5974, doi:10.5194/acp-8-5957-2008, 2008. 24630

Schrijver, C. J., Livingston, W. C., Woods, T. N., and Mewaldt, R. A.: The minimal solar activity in 2008–2009 and its implications for long-term climate modeling, *Geophys. Res. Lett.*, 38, L06701, doi:10.1029/2011GL046658, 2011. 24604

5 Shapiro, A. I., Schmutz, W., Schoell, M., Haberreiter, M., and Rozanov, E.: NLTE solar irradiance modeling with the COSI code, *Astron. Astrophys.*, 517, A48, doi:10.1051/0004-6361/200913987, 2010. 24584, 24589, 24636

10 Shapiro, A. I., Schmutz, W., Rozanov, E., Schoell, M., Haberreiter, M., Shapiro, A. V., and Nyeki, S.: A new approach to the long-term reconstruction of the solar irradiance leads to large historical solar forcing, *Astron. Astrophys.*, 529, A67, doi:10.1051/0004-6361/201016173, 2011. 24583, 24589, 24592

15 Shapiro, A. I., Schmutz, W., Dominique, M., and Shapiro, A.: Eclipses observed by LYRA – a sensitive tool to test the models for the solar irradiance, *Sol. Phys.*, doi:10.1007/s11207-012-0063-0, in press, 2012a. 24589

Shapiro, A. V., Shapiro, A. I., Dominique, M., Dammasch, I. E., Wehrli, C., Rozanov, E., and Schmutz, W.: Detection of solar rotational variability in the large yield radiometer (LYRA) 190–222 nm spectral band, *Sol. Phys.*, 121, doi:10.1007/s11207-012-0029-2, 2012b. 24589, 24590

20 Shchukina, N. and Trujillo Bueno, J.: The iron line formation problem in three-dimensional hydrodynamic models of solar-like photospheres, *Astrophys. J.*, 550, 970–990, doi:10.1086/319789, 2001. 24589

25 Snow, M., McClintock, W. E., Rottman, G., and Woods, T. N.: Solar stellar irradiance comparison experiment II (Solstice II): examination of the solar stellar comparison technique, *Sol. Phys.*, 230, 295–324, doi:10.1007/s11207-005-8763-3, 2005. 24593

Socas-Navarro, H.: A high-resolution three-dimensional model of the solar photosphere derived from Hinode observations, *Astron. Astrophys.*, 529, A37, doi:10.1051/0004-6361/201015805, 2011. 24584

30 Solanki, S. K. and Unruh, Y. C.: A model of the wavelength dependence of solar irradiance variations, *Astron. Astrophys.*, 329, 747–753, 1998. 24583, 24586

Solanki, S. K., Usoskin, I. G., Kromer, B., Schüssler, M., and Beer, J.: Unusual activity of the Sun during recent decades compared to the previous 11 000 years, *Nature*, 431, 1084–1087, doi:10.1038/nature02995, 2004. 24606

Title Page	Abstract	Introduction		
Conclusions	References			
Tables	Figures			
◀		▶		
◀		▶		
Back	Close			
Full Screen / Esc				
Printer-friendly Version				
Interactive Discussion				



- Solomon, S. D., Qin, D., Manning, M., Chen, Z., Marquis, M., Averyt, K. B., Tignor, M., and Miller, H.: Climate Change 2007: The Physical Science Basis, Contribution of Working Group I to the Fourth Assessment Report of the Intergovernmental Panel on Climate Change, Cambridge University Press, Cambridge, UK, 2007. 24560, 24595
- 5 SPARC-CCMVal: SPARC Report on the Evaluation of Chemistry-Climate Models, SPARC Report No. 5, WCRP-132, WMO/TD-No. 1526, edited by: Eyring, V., Shepherd, T. G., and Waugh, D. W., available at: www.atmosphysics.utoronto.ca/SPARC, last access: May 2011, 2010. 24594, 24596, 24604
- 10 Sperfeld, P., Metzdorf, J., Galal Yousef, S., Stock, K. D., and Möller, W.: Improvement and extension of the black-body-based spectral irradiance scale, *Metrologia*, 35, 267, doi:10.1088/0026-1394/35/4/9, 1998. 24572
- 15 Spruit, H. C.: Pressure equilibrium and energy balance of small photospheric fluxtubes, *Sol. Phys.*, 50, 269–295, doi:10.1007/BF00155292, 1976. 24580
- Spruit, H. C.: The flow of heat near a starspot, *Astron. Astrophys.*, 108, 356–360, 1982. 24580
- 20 Swartz, W. H., Stolarski, R. S., Oman, L. D., Fleming, E. L., and Jackman, C. H.: Middle atmosphere response to different descriptions of the 11-yr solar cycle in spectral irradiance in a chemistry-climate model, *Atmos. Chem. Phys. Discuss.*, 12, 7039–7071, doi:10.5194/acpd-12-7039-2012, 2012. 24562, 24599, 24600, 24602, 24630
- 25 Taylor, K. E., Stouffer, R. J., and Meehl, G. A.: An overview of CMIP5 and the experiment design, *B. Am. Meteorol. Soc.*, 93, 485–498, doi:10.1175/BAMS-D-11-00094.1, 2012. 24594, 24604
- Thuillier, G., Herse, M., Simon, P. C., Labs, D., Mandel, H., Gillotay, D., and Foujols, T.: The visible solar spectral irradiance from 350 to 850 nm as measured by the SOLSPEC spectrometer during the Atlas I mission, *Sol. Phys.*, 177, 41–61, 1998. 24586
- 30 Thuillier, G., Floyd, L., Woods, T. N., Cebula, R., Hilsenrath, E., Hersé, M., and Labs, D.: Solar irradiance reference spectra, in: *Solar Variability and its Effects on Climate*, Geophysical Monograph 141, edited by: Pap, J. M., Fox, P., Fröhlich, C., Hudson, H. S., Kuhn, J., McCormack, J., North, G., Sprigg, W., and Wu, S. T., American Geophysical Union, Washington DC, 171–194, 2004. 24571
- Thuillier, G., Foujols, T., Bolsée, D., Gillotay, D., Hersé, M., Peetermans, W., Decuyper, W., Mandel, H., Sperfeld, P., Pape, S., Taubert, D. R., and Hartmann, J.: SOLAR/SOLSPEC: scientific objectives, instrument performance and its absolute calibration using a blackbody as

[Title Page](#)[Abstract](#)[Introduction](#)[Conclusions](#)[References](#)[Tables](#)[Figures](#)[◀](#)[▶](#)[◀](#)[▶](#)[Back](#)[Close](#)[Full Screen / Esc](#)[Printer-friendly Version](#)[Interactive Discussion](#)

**Spectral irradiance
and climate**

I. Ermolli et al.

[Title Page](#)[Abstract](#)[Introduction](#)[Conclusions](#)[References](#)[Tables](#)[Figures](#)[◀](#)[▶](#)[◀](#)[▶](#)[Back](#)[Close](#)[Full Screen / Esc](#)[Printer-friendly Version](#)[Interactive Discussion](#)

- Vernazza, J. E., Avrett, E. H., and Loeser, R.: Structure of the solar chromosphere, III – models of the EUV brightness components of the quiet-sun, *Astrophys. J. Suppl.*, 45, 635–725, doi:doi:10.1086/190731, 1981. 24584
- 5 Vieira, L. E. A., Solanki, S. K., Krivova, N. A., and Usoskin, I.: Evolution of the solar irradiance during the Holocene, *Astron. Astrophys.*, 531, A6, doi:10.1051/0004-6361/201015843, 2011. 24583
- Viereck, R., Puga, L., McMullin, D., Judge, D., Weber, M., and Tobiska, W. K.: The Mg II index: a proxy for solar EUV, *Geophys. Res. Lett.*, 28, 1343–1346, doi:10.1029/2000GL012551, 2001. 24566, 24573
- 10 Vögler, A.: On the effect of photospheric magnetic fields on solar surface brightness, Results of radiative MHD simulations, *Mem. Soc. Astron. Ital.*, 76, 842–849, 2005. 24584
- Weber, M., Burrows, J. P., and Cebula, R. P.: Gome solar UV/VIS irradiance measurements between 1995 and 1997 – first results on proxy solar activity studies, *Sol. Phys.*, 177, 63–77, 1998. 24565
- 15 Weber, M., Pagaran, J., Dikty, S., von Savigny, C., Burrows, J., DeLand, M., Floyd, L., Harder, J., Mlynczak, M., and Schmidt, H.: Investigation of solar irradiance variations and their impact on middle atmospheric ozone, chapt. 3, in: Climate and Weather of the Sun-Earth System (CAWSES): Highlights from a Priority Program, edited by: Lübken, F.-J., Springer, Dordrecht, The Netherlands, 39–54, 2013. 24567
- 20 Wenzler, T., Solanki, S. K., Krivova, N. A., and Fluri, D. M.: Comparison between KPVT/SPM and SoHO/MDI magnetograms with an application to solar irradiance reconstructions, *Astron. Astrophys.*, 427, 1031–1043, doi:10.1051/0004-6361:20041313, 2004. 24579, 24583
- 25 Wenzler, T., Solanki, S. K., and Krivova, N. A.: Can surface magnetic fields reproduce solar irradiance variations in cycles 22 and 23?, *Astron. Astrophys.*, 432, 1057–1061, doi:10.1051/0004-6361:20041956, 2005. 24579, 24583
- Wenzler, T., Solanki, S. K., Krivova, N. A., and Fröhlich, C.: Reconstruction of solar irradiance variations in cycles 21–23 based on surface magnetic fields, *Astron. Astrophys.*, 460, 583–595, doi:10.1051/0004-6361:20065752, 2006. 24579, 24583
- 30 Wenzler, T., Solanki, S. K., and Krivova, N. A.: Reconstructed and measured total solar irradiance: is there a secular trend between 1978 and 2003?, *Geophys. Res. Lett.*, 36, L11102, doi:10.1029/2009GL037519, 2009. 24588
- Willson, R. C.: Active cavity radiometer type IV, *Appl. Optics*, 18, 179–188, doi:10.1364/AO.18.000179, 1979. 24575, 24629

Spectral irradiance and climate

I. Ermolli et al.

[Title Page](#)[Abstract](#)[Introduction](#)[Conclusions](#)[References](#)[Tables](#)[Figures](#)[◀](#)[▶](#)[◀](#)[▶](#)[Back](#)[Close](#)[Full Screen / Esc](#)[Printer-friendly Version](#)[Interactive Discussion](#)

- Willson, R. C. and Helizon, R. S.: EOS/ACRIM III instrumentation, in: Society of Photo-Optical Instrumentation Engineers (SPIE) Conference Series, vol. 3750 of Society of Photo-Optical Instrumentation Engineers (SPIE) Conference Series, edited by: Barnes, W. L., Proc. SPIE Vol. 3750, 233–242, Earth Observing Systems IV, Society of Photo-Optical Instrumentation Engineers (SPIE), Bellingham WA, USA, 233–242, 1999. 24629
- Willson, R. C., Gulkis, S., Janssen, M., Hudson, H. S., and Chapman, G. A.: Observations of solar irradiance variability, *Science*, 211, 700–702, doi:10.1126/science.211.4483.700, 1981. 24560, 24564, 24582
- WMO: Global Ozone Research and Monitoring Project Report No. 52, in: Scientific Assessment of Ozone Depletion: 2010, World Meteorological Organisation, Geneva, Switzerland, 516 pp., 2011. 24595
- Woods, T.: Solar irradiance variability: comparisons of observations over solar cycles 21–24, in: EGU General Assembly Conference Abstracts, vol. 14 of EGU General Assembly Conference Abstracts, edited by: Abbasi, A. and Giesen, N., Geophysical Research Abstracts, Vol. 14, EGU2012-1520, 2012, European Geosciences Union, Munich, Germany, 1520 pp., 2012. 24570, 24632
- Woods, T. N. and Rottman, G. J.: Solar ultraviolet variability over time periods of aeronomical interest, in: Atmospheres in the Solar System: Comparative Aeronomy, vol. 130 of AGU Monographs, edited by: Mendillo, M., Nagy, A., and Waite, J. H., AGU, Washington DC, doi:10.1029/130GM14, 221, 2002. 24632
- Woods, T. N., Prinz, D. K., Rottman, G. J., London, J., Crane, P. C., Cebula, R. P., Hilsenrath, E., Brueckner, G. E., Andrews, M. D., White, O. R., VanHoosier, M. E., Floyd, L. E., Herring, L. C., Knapp, B. G., Pankratz, C. K., and Reiser, P. A.: Validation of the UARS solar ultraviolet irradiances: comparison with the ATLAS 1 and 2 measurements, *J. Geophys. Res.*, 101, 9541–9570, doi:10.1029/96JD00225, 1996. 24565, 24586
- Woods, T. N., Tobiska, W. K., Rottman, G. J., and Worden, J. R.: Improved solar Lyman α irradiance modeling from 1947 through 1999 based on UARS observations, *J. Geophys. Res.*, 105, 27195–27216, doi:10.1029/2000JA000051, 2000. 24565
- Zhong, W., Osprey, S. M., Gray, L. J., and Haigh, J. D.: Influence of the prescribed solar spectrum on calculations of atmospheric temperature, *Geophys. Res. Lett.*, 35, L22813, doi:10.1029/2008GL035993, 2008. 24597

Title Page	
Abstract	Introduction
Conclusions	References
Tables	Figures
◀	▶
◀	▶
Back	Close
Full Screen / Esc	
Printer-friendly Version	
Interactive Discussion	



Spectral irradiance
and climate

I. Ermolli et al.

Table 1. Summary of main TSI measurements from space.

Spacecraft	Instrument	Start	End	Mean and st.dev. (Wm ⁻²)	Reference
NIMBUS	HF	Nov 1978	Dec 1993	1372.1 ± 0.8	Hickey et al. (1980)
SMM	ACRIM-I	Feb 1980	Jul 1989	1367.5 ± 0.7	Willson (1979)
ERBS	ERBE	Oct 1984	Mar 2003	1365.4 ± 0.6	Lee et al. (1987)
UARS	ACRIM-II	Oct 1990	Nov 2001	1364.4 ± 0.5	Pap et al. (1994)
SOHO	VIRGO	Feb 1996		1365.7 ± 0.6	Fröhlich et al. (1997)
ACRIM-sat	ACRIM-III	Apr 2000		1366.2 ± 0.7	Willson and Helizon (1999)
SORCE	TIM	Mar 2003		1360.9 ± 0.4	Lawrence et al. (2000)
PICARD	PREMOS	Nov 2010		1360.5 ± 0.4	Schmutz et al. (2009)

[Title Page](#)[Abstract](#)[Introduction](#)[Conclusions](#)[References](#)[Tables](#)[Figures](#)[|◀](#)[▶|](#)[◀](#)[▶](#)[Back](#)[Close](#)[Full Screen / Esc](#)[Printer-friendly Version](#)[Interactive Discussion](#)

Spectral irradiance and climate

I. Ermolli et al.

Table 2. Overview of atmospheric chemistry-climate models and the respective experimental designs using the NRLSSI and/or the SORCE data to study the atmospheric impact.

Model	Horizontal resolution	Top level	Number of vertical layers	Ozone interactively calculated	QBO	Length of simulation	Equilibrium simulation	Reference
SORCE/SIM comparison								
EMAC-FUB (ECHAM5/MESSy in FUB configuration)	T42	0.01 hPa	39	no	no	50 yr	perpetual Jan	Oberländer et al. (2012)
GEOSS CCM (using GEOS5)	2.5° × 2.5°	0.01 hPa	72	yes	no	25 yr	yes	Swartz et al. (2012)
HadGEM3	1.875° × 1.25°	85 km	85	no	yes	80 yr	yes	Ineson et al. (2011)
IC2-D	S 9.5° lat	0.26 hPa for chemistry	17 for chemistry	yes	no	670 days	yes	Haigh et al. (2010)
SOCOL v2.0	T30	0.01 hPa	39	yes	nudged	62 months	transient run (2004–2007)	Schranner et al. (2008)
WACCM	2.5° × 1.89°	0.000006 hPa	66	yes	yes	25 yr	yes	Merkel et al. (2011)
CMIP5 simulations								
HadGEM2	1.875° × 1.25°	85 Km	60	no	no	3 historical ens. (1850–2005)	no	Hardiman et al. (2012)
MPI-ESM-LR (atmospheric component: ECHAM6)	T63	0.01 hPa	47	prescribed solar induced ozone variation	no	3 historical ens. (1850–2005)	no	H. Schmidt (personal communica- tion, 2012)
WACCM'	2.5° × 1.89°	0.000006 hPa	66	no	yes	3 historical ens. (1850–2005)	no	D. R. Marsh (personal communica- tion, 2012)

[Title Page](#)

[Abstract](#)

[Introduction](#)

[Conclusions](#)

[References](#)

[Tables](#)

[Figures](#)

◀

▶

◀

▶

[Back](#)

[Close](#)

[Full Screen / Esc](#)

[Printer-friendly Version](#)

[Interactive Discussion](#)



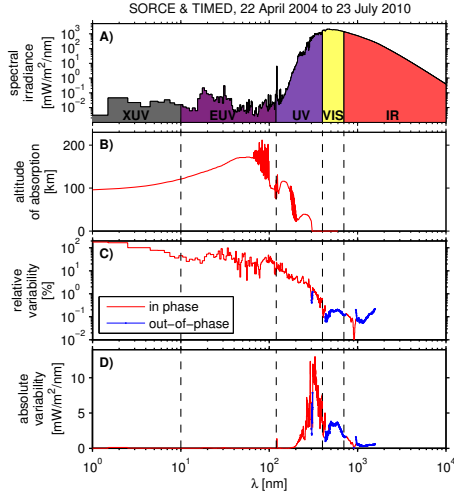


Fig. 1. The solar spectral irradiance as inferred from SORCE and TIMED observations only, from 22 April 2004 till 23 July 2010. **(A)** shows the average solar spectral irradiance for that period. A black-body model has been used to extend the SSI for wavelengths beyond 1580 nm. **(B)** displays the characteristic altitude of absorption in the Earth's atmosphere for each wavelength, defined as the altitude at which the optical depth equals one. **(C)** shows the relative variability (peak to peak/average) for solar cycle variations inferred from measurements obtained between 22 April 2004 and 23 July 2010. Spectral regions, where the variability is in phase with the solar cycle (represented by, e.g. the sunspot number or the TSI) are marked in red, while blue denotes ranges where the variability measured by SORCE is out-of-phase with the solar cycle. These phases, as well as the magnitude of the variability in the UV, are not all reproduced by models and other observations (see Sect. 3 as well as Figs. 2, 7 and 8), and thus should be considered with care. **(D)** shows the absolute variability, which peaks strongly in the near-UV.

Spectral irradiance and climate

I. Ermolli et al.

[Title Page](#)

[Abstract](#)

[Introduction](#)

[Conclusions](#)

[References](#)

[Tables](#)

[Figures](#)

[◀](#)

[▶](#)

[◀](#)

[▶](#)

[Back](#)

[Close](#)

[Full Screen / Esc](#)

[Printer-friendly Version](#)

[Interactive Discussion](#)



Spectral irradiance and climate

I. Ermolli et al.

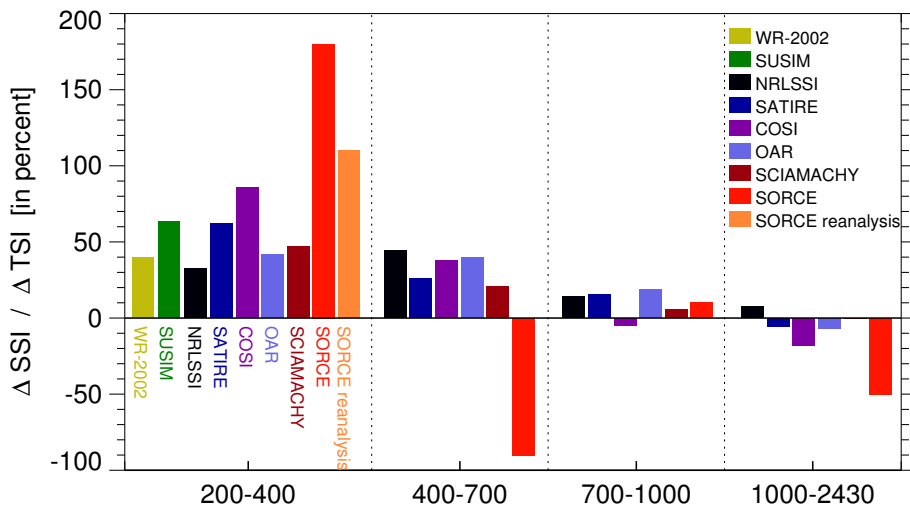


Fig. 2. Relative contribution of the UV (200–400 nm), visible (400–700 nm), near-IR (700–1000 nm) and IR (1000–2430 nm) ranges to the TSI change over the same period as derived from measurements and models described in Sects. 2 and 3. For SORCE/SIM, only the period between 2004 and 2008 can be considered. For other data and models, the plotted relative differences are between solar maximum and minimum. Within each wavelength bin, from left to right: WR-2002 (light green, only in UV; Woods and Rottman, 2002), UARS/SUSIM (green, only in UV; Morrill et al., 2011a), NRLSSI (black), SATIRE-S (blue), COSI (purple), OAR (light blue), SCIAMACHY (brown), SORCE (red), and SORCE re-analysis (orange, only in UV; Woods, 2012). The exact wavelength ranges used for SUSIM and SCIAMACHY in the UV are 150–400 nm and 240–400 nm, respectively. The possible related corrections are, however, expected to lie within 2–3 %. Note that for the SCIAMACHY-based model, the original values listed by Pagaran et al. (2009) are shown. As discussed by Krivova and Solanki (2013), these values should most likely be corrected by a factor of roughly 1.2 (see Sect. 3.1).

Title Page	Abstract	Introduction
Conclusions	References	
Tables	Figures	
Discussion Paper		
◀	▶	
◀	▶	
Back	Close	
Full Screen / Esc		
Printer-friendly Version		
Interactive Discussion		



**Spectral irradiance
and climate**

I. Ermolli et al.

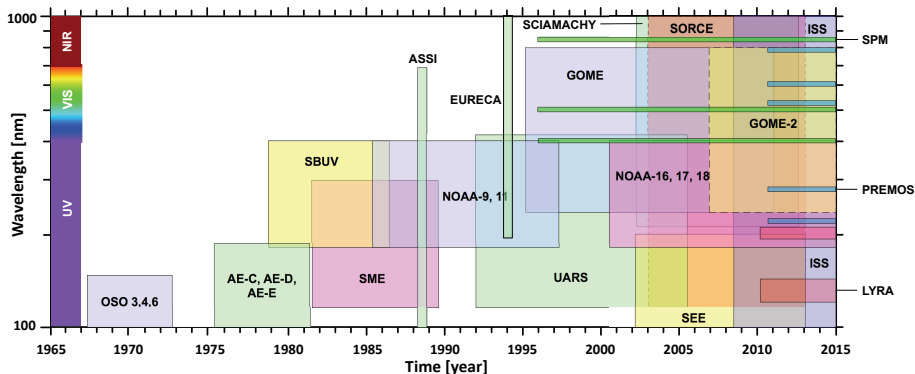


Fig. 3. Overview of the main satellite missions that have made SSI observations at wavelengths higher than 100 nm. Short missions such as sounding rockets are not indicated.

Title Page	
Abstract	Introduction
Conclusions	References
Tables	Figures
◀	▶
◀	▶
Back	Close
Full Screen / Esc	
Printer-friendly Version	
Interactive Discussion	



**Spectral irradiance
and climate**

I. Ermolli et al.

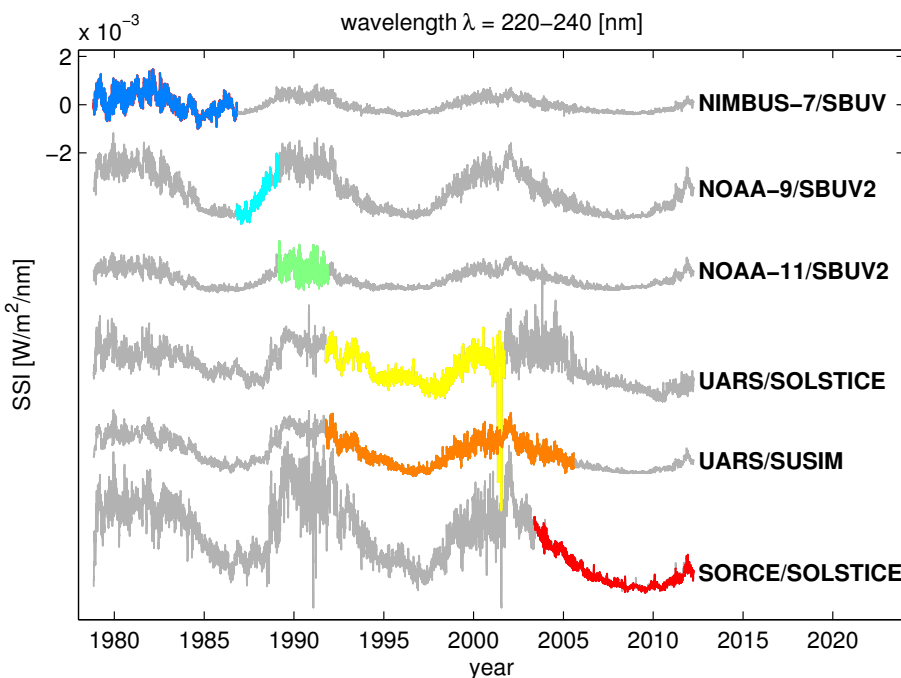


Fig. 4. Daily averages of the spectral irradiance in the 220–240 nm band, as measured by 6 different (and only partly overlapping) instruments. Each record has been shifted vertically for easier visualisation. Extrapolations are shown in grey, observations in colour. One- σ confidence intervals for the former are not shown here but are typically $0.4 \times 10^{-3} (\text{W m}^{-2} \text{ nm}^{-1})$.

[Title Page](#)[Abstract](#)[Introduction](#)[Conclusions](#)[References](#)[Tables](#)[Figures](#)[◀](#)[▶](#)[◀](#)[▶](#)[Back](#)[Close](#)[Full Screen / Esc](#)[Printer-friendly Version](#)[Interactive Discussion](#)

**Spectral irradiance
and climate**

I. Ermolli et al.

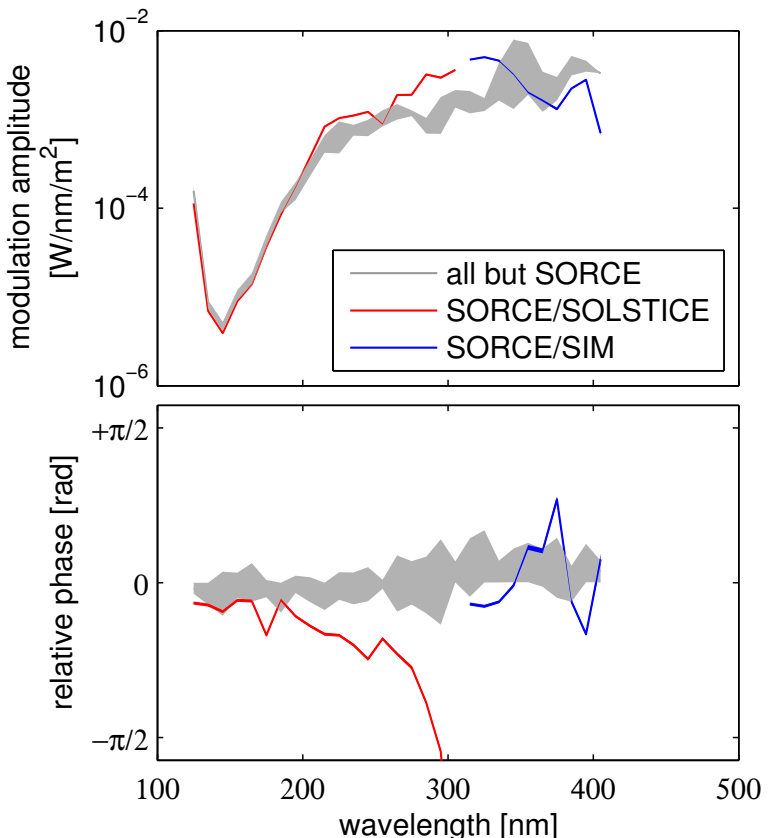


Fig. 5. Modulation amplitude (top) and phase (bottom) from SORCE/SIM and SORCE/SOLSTICE, compared to that from other instruments. The SSI has been averaged over 10 nm bins. The vertical width of the shaded area reflects the dispersion of the instruments ($\pm\sigma$ confidence interval).



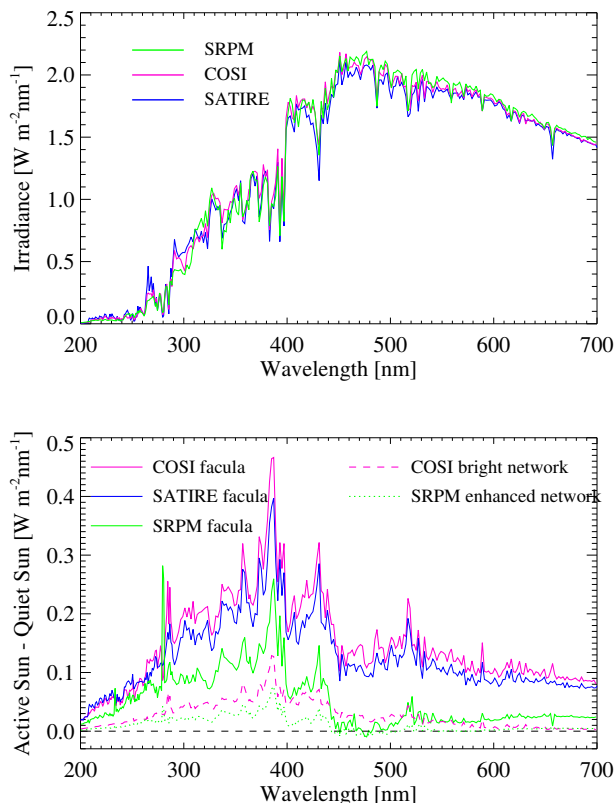


Fig. 6. Brightness of the quiet Sun (QS; top panel) and brightness contrasts of bright active components (bottom panel) in different models: SRPM (Fontenla et al., 2011, green lines), COSI (Shapiro et al., 2010, purple) and SATIRE (Unruh et al., 1999, blue). Note that contrasts depend on the position on the disc. Shown are averages over the entire disc under the assumption of a homogeneous spatial distribution of features.

[Title Page](#)[Abstract](#)[Introduction](#)[Conclusions](#)[References](#)[Tables](#)[Figures](#)[|◀](#)[▶|](#)[◀](#)[▶](#)[Back](#)[Close](#)[Full Screen / Esc](#)[Printer-friendly Version](#)[Interactive Discussion](#)

Spectral irradiance and climate

I. Ermolli et al.

Title Page

Abstract

act Introduction

Conclusion

ions References

Tables

Figures

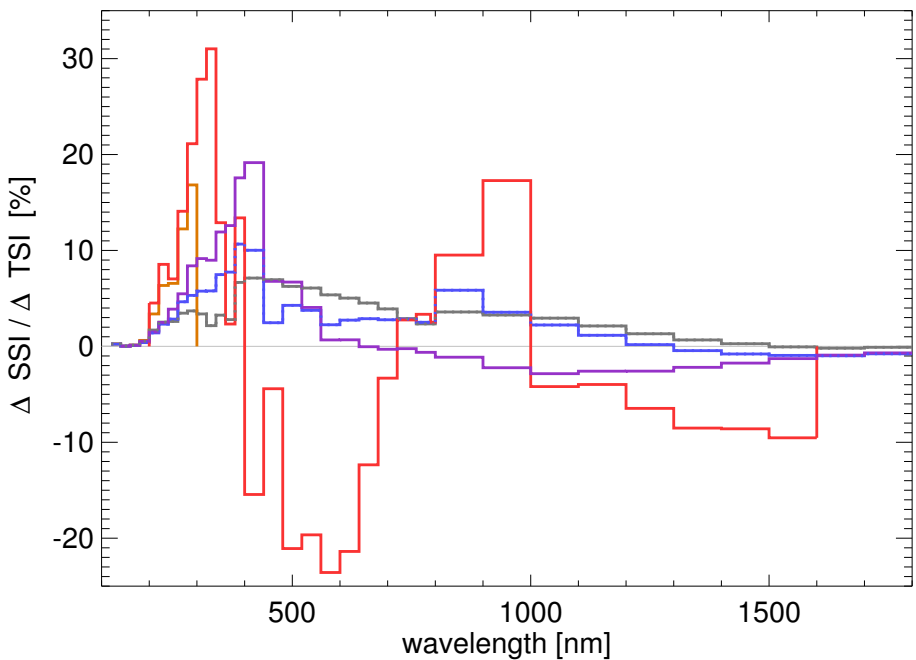


Fig. 7. Ratio of SSI variability to TSI variability between 200 nm and 1800 nm in bins of 20 nm below 400 nm, 40 nm in the range 400–800 nm, and 100 nm in the IR above 800 nm. Shown are SORCE/SOLSTICE (orange) and SORCE/SIM (red) measurements between 2004 and 2008, as well as the NRLSSI (grey), SATIRE-S (blue) and COSI (purple) models between the maximum and minimum of cycle 23.

Spectral irradiance and climate

I. Ermolli et al.

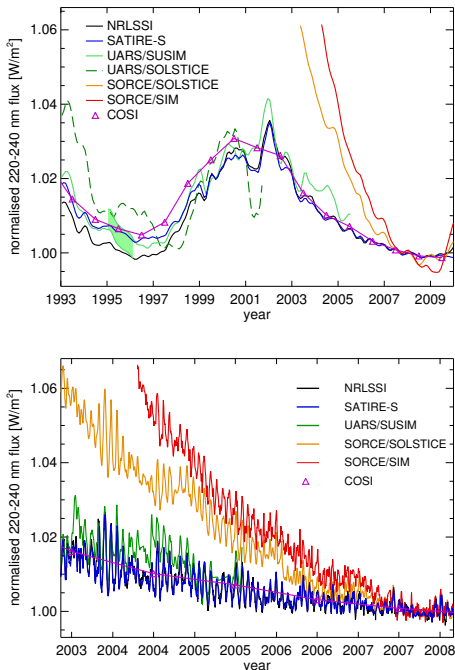


Fig. 8. Solar UV irradiance between 220 and 240 nm calculated with NRLSSI (black), SATIRE-S (blue) and COSI (magenta), and measured with UARS/SUSIM (darker green), UARS/SOLSTICE (light green), SORCE/SOLSTICE (orange) and SORCE/SIM (red). The pale green shading in the upper panel marks the period when the sensitivity of the UARS/SUSIM instrument (and thus the flux) changed, so that a shift was applied to the data before that (see Krivova et al., 2006, 2009 for details). Top panel shows 3-month smoothed values over the period 1993–2009, while the bottom panel is limited to the period when SORCE was in operation, i.e. after 2003, and shows daily values, except for the COSI model, for which only yearly averages are available. All quantities are normalized to the corresponding mean values during the last activity minimum (2009).

Title Page

Abstract

Introduction

Conclusions

s References

Tables

Figures

Page 1

Page 1



Back

Close

Full Screen / Esc

[Printer-friendly version](#)

Interactive Discussion



Spectral irradiance and climate

I. Ermolli et al.

[Title Page](#)

[Abstract](#)

[Introduction](#)

[Conclusions](#)

[References](#)

[Tables](#)

[Figures](#)

[◀](#)

[▶](#)

[◀](#)

[▶](#)

[Back](#)

[Close](#)

[Full Screen / Esc](#)

[Printer-friendly Version](#)

[Interactive Discussion](#)

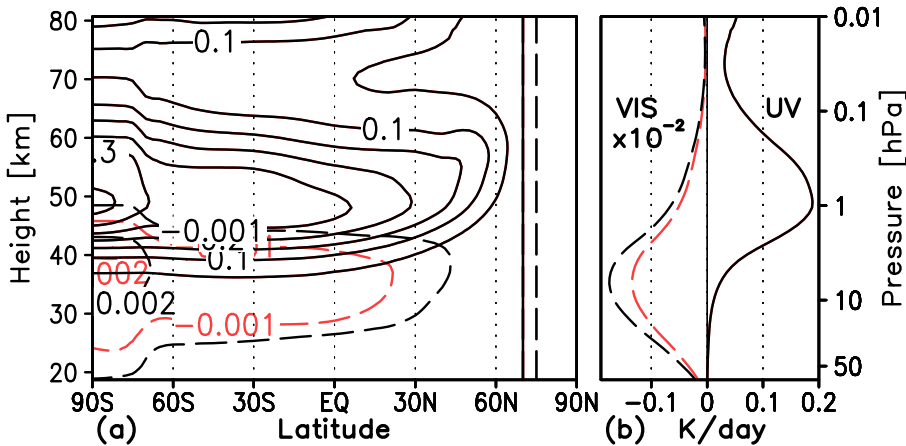


Fig. 9. Updated from Oberländer et al. (2012) **(a)** Difference in zonal mean solar heating rates between 2004 and 2007 in K day^{-1} from the SIM data, and **(b)** difference in the global mean 2004–2007 solar heating rate signal between SORCE/SIM and NRLSSI data. Solid lines denote the UV spectral range, and dashed lines denote the VIS spectral range. Red dashed lines in panels **(a)** and **(b)** denote the same differences in zonal and global mean, as calculated and presented in Figs. 3b, c in Oberländer et al. (2012); black dashed lines indicate the enhanced solar signal in the VIS range, when extending the spectral resolution of the FUBRad shortwave radiation code from one to six bands in the Chappuis bands.

Spectral irradiance and climate

I. Ermolli et al.

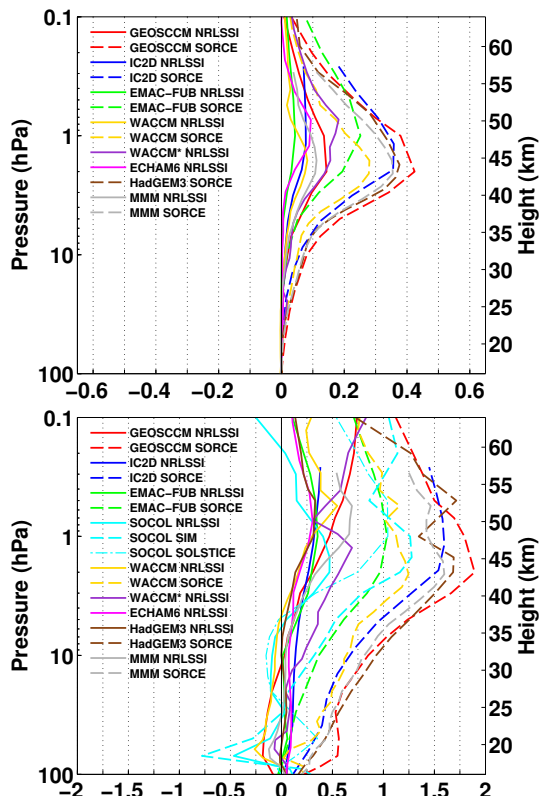


Fig. 10. Differences for January between 2004 and 2007 averaged over the tropics from 25° S to 25° N for different atmospheric models using the NRSSI data (solid lines) and the SORCE/SIM and SORCE/SOLSTICE data (dashed lines) for (a) the shortwave heating rate in Kelvin per day (Kday^{-1}) and (b) the temperature in Kelvin (K). For details please see text.

[Title Page](#)

[Abstract](#)

[Introduction](#)

[Conclusions](#)

[References](#)

[Tables](#)

[Figures](#)

[◀](#)

[▶](#)

[◀](#)

[▶](#)

[Back](#)

[Close](#)

[Full Screen / Esc](#)

[Printer-friendly Version](#)

[Interactive Discussion](#)



**Spectral irradiance
and climate**

I. Ermolli et al.

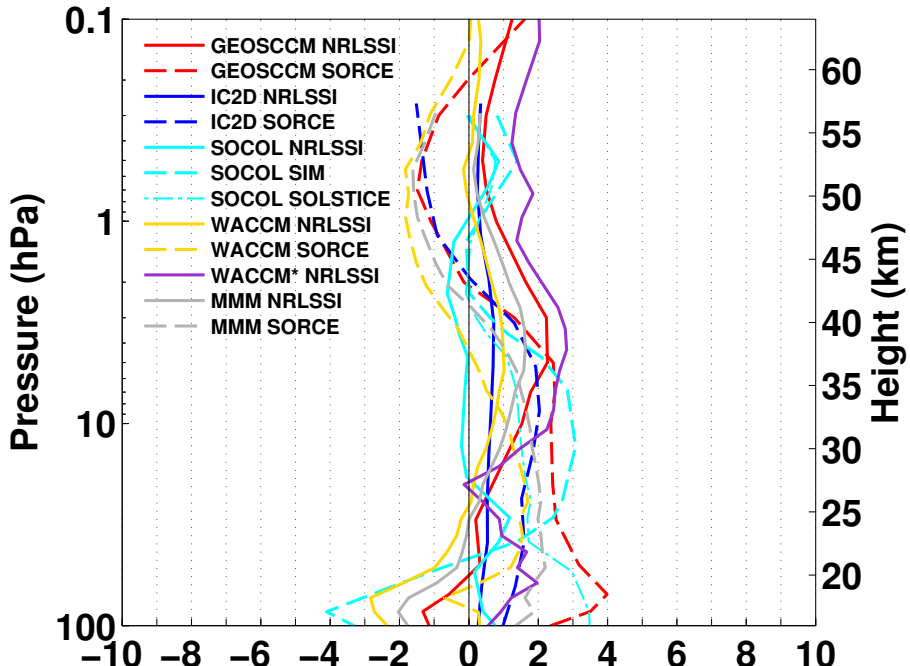
[Title Page](#)[Abstract](#)[Introduction](#)[Conclusions](#)[References](#)[Tables](#)[Figures](#)[◀](#)[▶](#)[◀](#)[▶](#)[Back](#)[Close](#)[Full Screen / Esc](#)[Printer-friendly Version](#)[Interactive Discussion](#)

Fig. 11. As Fig. 10 but for the ozone response in percent.

**Spectral irradiance
and climate**

I. Ermolli et al.

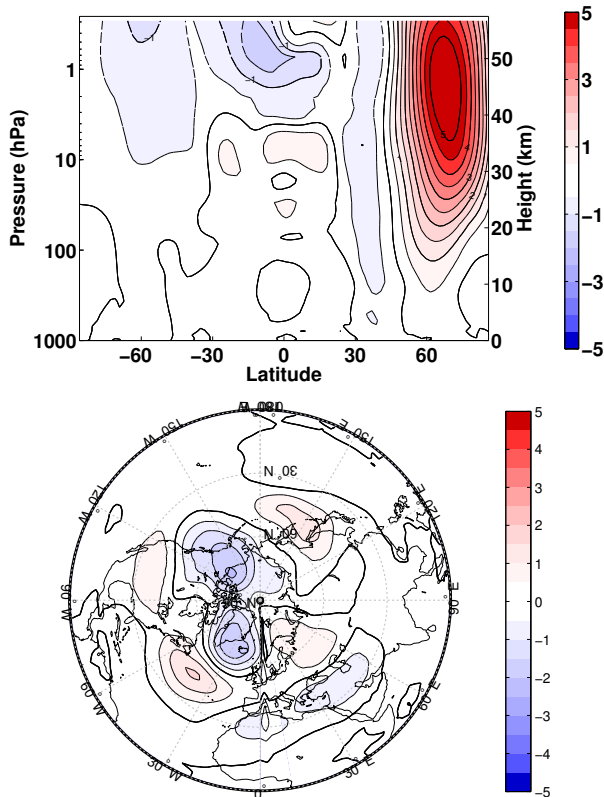


Fig. 12. Multi Model Mean (MMM) of the HadGEM3, the GEOS CCM, and the WACCM model for **(a)** the zonal mean zonal wind differences between 2004 and 2007 in January using the SORCE/SIM forcing, and **(b)** the corresponding geopotential height differences at 500 hPa.

Title Page	Abstract	Introduction
Conclusions	References	
Tables	Figures	
◀	▶	
◀	▶	
Back	Close	
Full Screen / Esc		
Printer-friendly Version		
Interactive Discussion		

